UNLOCKING THE FOREST INVENTORY AND ANALYSIS DATABASE:
APPLICATIONS TO NATION-WIDE FOREST HEALTH MONITORING

By

Hunter Stanke

A THESIS

Submitted to
Michigan State University
in partial fulfillment of the requirements
for the degree of

Forestry – Master of Science

2020

ABSTRACT

UNLOCKING THE FOREST INVENTORY AND ANALYSIS DATABASE:
APPLICATIONS TO NATION-WIDE FOREST HEALTH MONITORING

By

Hunter Stanke

Forest Inventory and Analysis (FIA) is a US Department of Agriculture Forest Service program that aims to monitor changes in forests across the US. FIA hosts one of the largest ecological datasets in the world, though its complexity limits access for many potential users. `rFIA` is an R package designed to simplify the estimation of forest attributes using data collected by the FIA Program. Specifically, `rFIA` improves access to the spatio-temporal estimation capacity of the FIA Database via space-time indexed summaries of forest variables within user-defined population boundaries. The package implements multiple design-based estimators, and has been validated against official estimates and sampling errors produced by the FIA Program. The package has been made open-source is freely available for download from the Comprehensive R Archive Network.

In recent decades, forests of the western US have experienced unprecedented change in climate and forest disturbance regimes, and widespread shifts in forest composition, structure, and function are expected in response. However, large-scale, comprehensive assessments of tree population performance have yet to be conducted in the region. We develop an index of forest population performance based on repeated censuses of field plots, and apply this index to assess the status of the most abundant tree species in the western US. Our study provides empirical evidence to suggest tree species in the western US are exhibiting strong divergence in population performance, with over half (70%) of species experiencing range-wide population decline. We found spatial variation in population performance across the ranges of all species, indicating range shifts are already underway. Our results further indicate that species decline can seldom be attributed to a single forest disturbance agent, highlighting the importance of considering multiple risks factors in broad-scale forest management.

ACKNOWLEDGEMENTS

TABLE OF CONTENTS

LIST OF TABLES

LIST OF FIGURES

CHAPTER 1

RFIA: AN R PACKAGE FOR ESTIMATION OF FOREST ATTRIBUTES WITH THE US FOREST INVENTORY AND ANALYSIS DATABASE

1.1 Introduction

Forest Inventory and Analysis (FIA) is a United States Department of Agriculture Forest Service program with the goal of monitoring and projecting changes in forests across the United States (US) [USDA Forest Service, 2019a]. The program collects, publishes, and analyzes data describing the extent, condition, volume, growth, and use of trees from all land ownerships in the nation, with some records dating back to the early 1930s [Tinkham et al., 2018, Smith, 2002]. In 1999, the FIA program established a systematic grid of permanent ground plots that are evenly divided into panels measured in a continuous cycle, allowing spatially unbiased estimates of forest attributes to be computed on an annual basis [Gillespie, 1999, Smith, 2002]. The flexibility inherent to the FIA inventory system creates unprecedented opportunities to assess forest change across space, through time, and within unique populations of interest [Tinkham et al., 2018, Gray et al., 2012].

The research significance of the FIA program has increased in recent decades, with primary applications in carbon cycling, forest growth, forest health, and remote sensing [Tinkham et al., 2018]. The FIA program hosts one of the largest ecological datasets in the world by spatial and temporal extent [Tinkham et al., 2018], including records from over 5.8 million trees measured at least twice and encompassing a range of ecological diversity unmatched by any other large-scale national forest inventory system [Tomppo et al., 2010]. The breadth of attributes currently measured by the FIA program, ranging from forest composition and structure to soil chemistry and invasive species abundance, makes it a vast and powerful resource for monitoring the status and trends in forest attributes from the scale of individual trees to subcontinents [Tinkham et al., 2018].

The primary limitation for individuals using FIA data in their own analyses is the complex sample design, database structure, and Structured Query Language used by the FIA program [Tinkham et al., 2018, Kromroy et al., 2008]. FIA data are publicly available in several formats (e.g., FIA DataMart) and estimation is facilitated through online tools (e.g., EVALIDator) [USDA Forest Service, 2019b, Pugh et al., 2018] and a non-public R package, FIESTA [Frescino et al., 2015]. That said, FIA data are difficult for many non-FIA users to interpret and understand [Tinkham et al., 2018] and there is potential to increase the use of these incredibly rich data among industry professionals, academic scientists, and the general public. To promote use of this valuable public resource and extend the reach of the FIA program and the publicly available data, there is a need for a flexible, user-friendly tool that simplifies the process of working with FIA data for experts and novices alike. To this end, we developed `rFIA`, an add-on package for R [R Core Team, 2018b].

`rFIA` implements FIA's design-based estimation procedures [Bechtold et al., 2005] for over 50 forest attributes using a simple, yet powerful design. `rFIA` greatly improves access to the spatio-temporal estimation capacity inherent to the FIA program by allowing space-time indexed summaries of forest attributes to be produced within user-defined population boundaries (e.g., geographic, temporal, biophysical). The package enhances the value of FIA for temporal change detection and forest health monitoring by implementing five design-based estimators that offer flexibility in a balance between precision and temporal smoothing. Our intention in developing `rFIA` is to provide a versatile, user-friendly software that allows all R users to unlock the value of the FIA program.

1.2 Methods

1.2.1 Software design

We designed `rFIA` to be intuitive to use and support common data representations by directly integrating other popular R packages into our development. We achieve efficient joins, queries, and data summaries with the `dplyr` package [Wickham et al., 2015]. Specifically,

Figure 1.1: Software availability

Name of software rFIA
Type of software Add-on package for R
First available 2019
Program languages R
License GPL 3
Code Repository `https://cran.r-project.org/web/packages/rFIA/index.html`
Installation in R `install.packages("rFIA")`
Developers Hunter Stanke, Andrew O. Finley
Contact Address Department of Forestry,
        Michigan State University, East Lansing, MI, USA

we leverage `dplyr` for joining and filtering FIA tables, facilitating hierarchical grouping of summary attributes, and implementing non-standard evaluation in `rFIA` core functions. We achieve efficient space-time query and summary within user-defined population boundaries (i.e., spatial polygons) with the `sf` package [Pebesma, 2018]. Parallel processing is implemented with the `parallel` package [R Core Team, 2018a]. Parallel implementation is achieved using a snow type cluster [Tierney et al., 2018] on any Windows OS, and with multi-core forking [R Core Team, 2018a] on any Unix or Mac OS.

1.2.2 Sampling and estimation procedures

The design-based estimation procedures used by the FIA program and implemented by `rFIA` have been widely described in the literature [Bechtold et al., 2005, McRoberts et al., 2005a, Hoffman et al., 2014], and hence will only be briefly described here. All estimators for population totals, ratios, and associated variances are derived from the Horvitz-Thompson estimator and hence incorporate design information via inverse-probability weighting [Horvitz and Thompson, 1952]. Bechtold et al. [2005] describes in detail the theoretical basis for estimators used by the FIA program and implemented by `rFIA`.

The FIA program conducts forest inventories using a multi-phased sampling procedure designed to reduce variance through stratification [Bechtold et al., 2005, McRoberts et al., 2005a]. In the pre-field phase, remotely sensed imagery are used to stratify land area by

3

Figure 1.2: FIA ground plot design (left) and an example map of forested condition classes on a subplot (right).

Subplot:
24 ft radius

2

Macroplot:
58.9 ft radius

Distance between
subplot centers is
120 ft horizontal

Microplot:
6.8 feet radius center is
12 feet horizontal @ 90°
azimuth from the subplot
center

1

4

3

**Subplot 3
Condition Map**

Condition 1:
Oak-hickory
forest

Condition 2:
Pine plantation
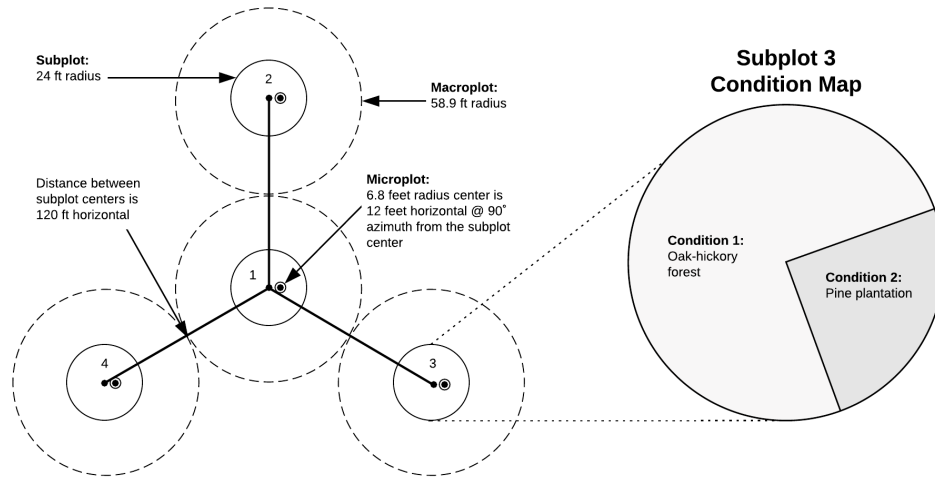
determining dominant land use in each pixel within the population of interest. In the core phase, permanent ground plots are systematically distributed across the US at a rate of approximately 1 plot per 6000 acres using a hexagonal sampling frame [Bechtold et al., 2005, McRoberts et al., 2005a]. Each plot is assigned to a single stratum based on the the pre-field stratification of the plot center. If any portion of a plot is determined to contain a forest land use from pre-field stratification, a field crew will visit the site and measure core FIA variables [Bechtold et al., 2005]. In the intensive phase, additional forest and ecosystem health variables are measured on 5-15% of established core plots (approximately 1 plot per 96,000 acres).

FIA permanent ground plots consist of clusters of four subplots (Figure 1.2), where tree attributes are measured for all stems 5.0 inches diameter at breast height (DBH) and larger. Within each subplot, a microplot is established where tree attributes are measured for saplings (1.0-4.9 inches DBH). Each subplot is surrounded by a macroplot, on which rare events such as large trees are optionally measured. In addition to tree attributes, data are collected that describe the area where trees are located on each subplot and macroplot. If area attributes (e.g., ownership group, forest type, stocking) vary substantially across a plot,

the land area within the plot is divided into distinct domains referred to as condition classes so that tree data can be properly associated with area classifications (Figure 1.2).

Plot-level estimates of forest attributes (e.g., tree biomass, forested area) are obtained by summing observations or estimates of the attribute, which are within the population of interest (e.g., live trees, private land), across the plot. Observations are multiplied by 1 if the attribute is within the population of interest, and 0 otherwise. Thus if all observations on a plot fall outside the population of interest, observations will sum to 0 for the plot. For ratio estimates (e.g., tree biomass per unit area), it is possible to specify different populations of interest for the numerator and denominator attributes.

The FIA program uses an annual panel system to estimate both current inventory and change. Individual panels are represented by a subset of ground plots that are measured in the same year and represent complete spatial coverage across the population of interest [McRoberts and Miles, 2016]. In the eastern US, inventory cycles consist of 5 or 7 annual panels, with 20 or 15 percent of ground plots measured in each year, respectively. In the western US, inventory cycles include 10 annual panels and thus 10 percent of ground plots are measured each year [Bechtold et al., 2005]. Variance reduction can often be achieved by combining current panels with data from previous panels, although FIA does not prescribe a core procedure for panel combination because a single approach is unlikely to be suitable for all estimation objectives or across a wide variety of spatial, temporal, and population conditions [Bechtold et al., 2005].

In rFIA, users may choose from one of four unique estimators that combine data from multiple panels or choose to return estimates from individual annual panels (ANNUAL), thereby forgoing panel combination entirely. The "temporally-indifferent" (TI) estimator is used by default, essentially pooling all panels within an inventory cycle into a large periodic inventory. The TI estimator is commonly used by other FIA estimation tools, like EVAL-IDator [USDA Forest Service, 2019b, Pugh et al., 2018]. Alternatively, individual panels may be weighted by employing a moving-average estimator, including the simple moving

average (SMA), linear moving average (LMA), or exponential moving average (EMA). The SMA applies equal weight to all annual panels (Eq. 1.1), while the LMA and EMA apply weights that decay linearly or exponentially as a function of time since measurement, respectively (Eq. 1.2-1.3). In each case of the moving average, panel weights sum to one across an inventory cycle. Panel weights are computed as follows:

$$w_{p,SMA} = \frac{1}{N} \tag{1.1}$$

$$w_{p,LMA} = \frac{p}{\sum_{i=1}^{N} p_i} \tag{1.2}$$

$$w_{p,EMA} = \frac{\lambda(1-\lambda)^{1-p}}{\sum_{i=1}^{N} \lambda(1-\lambda)^{1-p_i}} \tag{1.3}$$

where w_p is the constant positive weight for annual panel, p, described as the sequential index of the panel within an inventory cycle (i.e., $p = 1, 2, \ldots, N$), N is the total number of annual panels in the inventory cycle, and λ is a decay parameter, ranging between zero and one, that controls the behavior of the exponential weighting function (Eq. 3). As λ approaches 1, panel weights become nearly evenly distributed across the inventory cycle, and estimates produced by the EMA will approach those of the SMA. As λ approaches 0, weights are skewed towards the most recent panel and estimates of the EMA will approach those of individual annual panels. The inclusion of λ makes the EMA the most versatile estimator offered in `rFIA`.

In general, sample variance is minimized when panel weights are evenly distributed across the inventory cycle (e.g., SMA), with the trade-off of introducing temporal lag-bias by weighting recent measurements the same as older measurements. Hence, equal weighting schemes could be undesirable in settings where variable values change over time. Alternatively, applying lower weights to less recent panels reduces the effective sample size of the inventory, effectively increasing variance but reducing temporal smoothing by favoring more recent measurements. We advise users of `rFIA` to be aware of this trade-off between precision and temporal smoothing when considering various estimators offered in the package.

Table 1.1: Comparison of estimates produced by rFIA and EVALIDator for select forest attributes. Estimates from both tools were produced using the "temporally-indifferent" estimator.

Forest Attribute	rFIA		EVALIDator	
	Estimate	*SE*	*Estimate*	*SE*
Live tree abundance ($trees/acre$)	432.63	4.46	432.63	4.46
Live tree basal area ($ft^2/acre$)	121.19	2.13	121.19	2.13
Live tree merchantable volume ($ft^3/acre$)	2625.99	2.65	2625.99	2.65
Live tree sawlog volume ($ft^3/acre$)	1648.77	3.56	1648.77	3.56
Live tree aboveground biomass ($tons/acre$)	75.99	2.38	75.99	2.38
Live tree aboveground carbon ($tons/acre$)	37.99	2.38	37.99	2.38
Annual net biomass growth ($tons/acre/year$)*	1.06	6.39	1.06	6.39
Annual mortality ($trees/acre/year$)*	1.47	6.93	1.47	6.93
Annual removals ($trees/acre/year$)*	0.36	31.09	0.36	31.09
Coarse woody material volume ($ft^3/acre$)	299.87	23.92	299.87	23.92
Coarse woody material biomass ($tons/acre$)	3.08	25.25	3.08	25.25
Coarse woody material carbon ($tons/acre$)	1.52	25.14	1.52	25.14
Total forest area ($acres\ x\ 10^{-3}$)	1789.61	2.29	1789.61	2.29

1.2.3 Software testing

We have conducted extensive validation for all estimated attributes for small and large areas against EVALIDator [USDA Forest Service, 2019b]. Here we present an abbreviated version of a validation for the state of Connecticut in the year 2018 using the "temporally-indifferent" estimator (Table 1.1). Current status estimates were produced for live trees with DBH $\geq$ 1.0 inch and annual change estimates were produced for all stems with DBH $\geq$ 5.0 inches. Down woody material estimates were produced for the 1000 hour fuel class (coarse woody debris). Total forest area estimates were produced using plots containing a forested condition. All estimates and associated sampling errors produced by rFIA match those produced by EVALIDator. A detailed description of the validation described in Table 1.1, including code used to produce estimates using rFIA, can be found in Appendix A.

Table 1.2: List of core functions available within `rFIA`.

Function	Description
`area`	Estimate land area in various classes
`biomass`	Estimate volume, biomass, and carbon stocks of standing trees
`clipFIA`	Spatial and temporal queries for FIA data
`diversity`	Estimate species diversity
`dwm`	Estimate volume, biomass, and carbon stocks of down woody material
`findEVALID`	Lookup Evaluation IDs (EVALIDs) by year and evaluation types
`getFIA`	Download FIA data, load into R, and optionally save to disk
`growMort`	Estimate recruitment, mortality, and harvest rates
`invasive`	Estimate areal coverage of invasive species
`plotFIA`	Produce static and animated plots of FIA summaries
`readFIA`	Load FIA database into R environment from disk
`seedling`	Estimate abundance of seedlings
`standStruct`	Estimate forest structural stage distributions
`tpa`	Estimate abundance of standing trees
`vitalRates`	Estimate live tree growth rates
`writeFIA`	Write in-memory FIA database to disk

1.3   `rFIA` package features

`rFIA` is capable of estimating more forest attributes from FIA data than any other publicly available tool and offers unmatched flexibility in defining unique populations of interest and producing space-time indexed summaries of forest attributes. Users can install the released version of `rFIA` from CRAN (v0.1.0, 28 October 2019), or alternatively install the development version from Github (https://github.com/hunter-stanke/rFIA) using `devtools` [Wickham et al., 2019]. Table 1.2 depicts a list of core functions available in `rFIA`. A schematic diagram for using `rFIA` to produce population estimates of forest attributes can be found in Figure 1.3.

1.3.1   Loading FIA data

Users can automatically download state subsets of the FIA database [USDA Forest Service, 2019b], load these data into R, and optionally save to disk using `getFIA`. Simply specify the state abbreviation code for the state(s) of interest as a character vector in the `states`

Figure 1.3: Schematic diagram of the features of `rFIA`: the blue boxes represent decision points for the user; green boxes represent data or results that are produced and/or processed by `rFIA` functions, which are represented in the orange boxes.
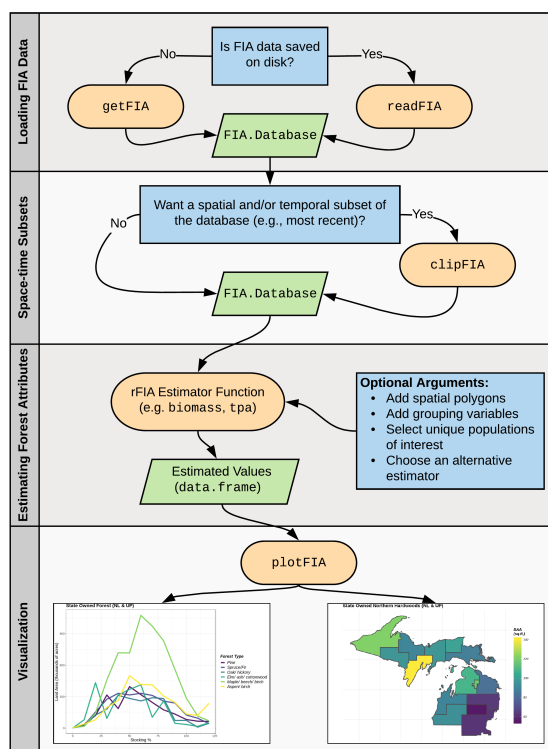
argument of `getFIA` (e.g., `states = "CT"` for Connecticut). Alternatively, `getFIA` can be used to download, load, and optionally save select table(s) contained in the FIA database by specifying the names of the tables of interest in the `tables` argument (e.g., `tables = c("TREE", "PLOT")` for the `TREE` and `PLOT` tables). All FIA data are downloaded from the FIA DataMart [USDA Forest Service, 2019b] and saved as comma-delimited text files in a local directory.

If FIA data are already saved on disk as comma-delimited text files, `readFIA` can be used to load these data into R. `readFIA` requires that FIA data files maintain original FIA naming conventions (as downloaded from the FIA DataMart) for referential integrity. All FIA data files should be stored in a single directory with no sub-directories for proper loading with `readFIA`. We recommend using `getFIA` to download and save new FIA data and `readFIA` to reload these data in future R sessions. All data loaded with `getFIA` or `readFIA` are stored

as a modified list object called a `FIA.Database`. All common list operations are valid for the `FIA.Database` object class, and individual FIA tables can be accessed using the `$` operator.

1.3.2 Spatial and temporal subsets

Spatial and/or temporal subsets of a `FIA.Database` may be implemented with `clipFIA` if users are interested in producing estimates for select areal regions and/or time periods contained within the spatial-temporal extent of the `FIA.Database`. Such subsets are not required to use `rFIA` estimator functions (listed in Table 1.3) to produce estimates of forest attributes. However, limiting the spatial and temporal extent of the query region will conserve memory and decrease processing time.

Users may subset a `FIA.Database` to the boundaries of a spatial polygon object by specifying the name of the spatial object in the `mask` argument of `clipFIA`. All spatial polygon classes from the `sp` and `sf` packages are supported. To obtain the most recent subset of a `FIA.Database` by reporting year, specify `mostRecent = TRUE` in `clipFIA` (TRUE by default). If a `FIA.Database` contains multiple states with different reporting schedules, setting `mostRecent = TRUE` will return the data necessary to produce estimates for the most recent reporting year in each state. Alternatively, users may specify `matchEval = TRUE` to obtain a subset of data associated with reporting years which are common among all states in the `FIA.Database`.

1.3.3 Estimating forest attributes

`rFIA` includes a range of estimator functions designed to produce population and plot-level estimates directly from `FIA.Database` objects. All estimator functions share a similar design, although minor nuances exist between functions due to variation in the forms of estimates they invoke (Table 1.3). We will demonstrate the functionality of `rFIA` estimator functions using `biomass`, a function designed to estimate volume, biomass, and carbon of standing trees.

Table 1.3: List of core arguments available in rFIA estimator functions.

	bySpecies	bySizeClass	treeDomain	areaDomain	tidy	method
area				*		*
biomass	*	*	*	*		*
diversity		*	*	*		*
dwm				*	*	*
growMort	*	*	*	*		*
invasive	(default)			*		*
seedling	*		*	*		*
standStruct				*	*	*
tpa	*	*	*	*		*
vitalRates	*	*	*	*		*

To produce population estimates for the region contained within the spatial extent of a `FIA.Database`, specify the name of the `FIA.Database` as the `db` argument of any `rFIA` estimator function (Figure 1.4). All `rFIA` estimator functions return population estimates and associated sampling errors for each reporting year in the `FIA.Database` by default. To return estimates at the plot-level, specify `byPlot = TRUE`. In this case, estimates will be returned for each occasion that an individual plot was measured.

1.3.3.1 Grouped Estimates

Often it is useful to produce estimates grouped by discrete categories, such as species, forest type, ownership group, or diameter class. `rFIA` estimator functions can produce estimates grouped by fields contained in the `PLOT`, `COND`, and `TREE` tables of a `FIA.Database`. To produce grouped estimates, specify the name(s) of fields representing the grouping variable(s) as the `grpBy` argument of any estimator function (Figure 1.5). If more than one grouping variable is provided to `grpBy`, grouping will occur hierarchically based on the order variable names are listed. In addition to `grpBy`, some `rFIA` estimator functions include `bySpecies` and `bySizeClass` arguments for convenience. Set either of these arguments as `TRUE` to produced estimates grouped by species and/or 2.0 inch DBH classes, respectively. Alternatively, users may specify `grpBy = SPCD` to group estiamtes by species and use the `makeClasses` function

Figure 1.4: Example code for producing basic population and plot-level estimates using `rFIA`.

```r
## Load state subset for Rhode Island,
## included with rFIA
data("fiaRI")
## Estimates for entire state
biomass(db = fiaRI)

# A tibble: 5 x 19
   YEAR NETVOL_ACRE SAWVOL_ACRE BIO_AG_ACRE BIO_BG_ACRE BIO_ACRE
  <int>       <dbl>       <dbl>       <dbl>       <dbl>    <dbl>
1  2014       2396.       1356.        68.0        13.5     81.6
2  2015       2438.       1385.        69.1        13.7     82.9
3  2016       2491.       1419.        70.6        14.0     84.6
4  2017       2500.       1422.        70.8        14.1     84.8
5  2018       2491.       1419.        70.4        14.0     84.4
# ... with 13 more variables: CARB_AG_ACRE <dbl>, CARB_BG_ACRE <dbl>,
#   CARB_ACRE <dbl>, NETVOL_ACRE_SE <dbl>, SAWVOL_ACRE_SE <dbl>,
#   BIO_AG_ACRE_SE <dbl>, BIO_BG_ACRE_SE <dbl>, BIO_ACRE_SE <dbl>,
#   CARB_AG_ACRE_SE <dbl>, CARB_BG_ACRE_SE <dbl>, CARB_ACRE_SE <dbl>,
#   nPlots_VOL <dbl>, nPlots_AREA <dbl>

## Plot-level estimates
biomass(db = fiaRI, byPlot = TRUE)

# A tibble: 352 x 11
   PLT_CN   YEAR NETVOL_ACRE SAWVOL_ACRE BIO_AG_ACRE BIO_BG_ACRE BIO_ACRE
    <dbl> <int>       <dbl>       <dbl>       <dbl>       <dbl>    <dbl>
1 1.45e14  2009           0           0           0           0        0
2 1.45e14  2009           0           0           0           0        0
3 1.45e14  2009           0           0           0           0        0
4 1.45e14  2009       2335.       1481.        70.4        13.6     84.0
5 1.45e14  2009       2760.       1690.        86.3        16.7     103.
# ... with 347 more rows, and 4 more variables: CARB_AG_ACRE <dbl>,
#   CARB_BG_ACRE <dbl>, CARB_ACRE <dbl>, nStems <int>
```

to define their own diameter classes. More information on variable definitions in the FIA Database can be found in the FIA Database Description and User Guide for Phase 2 [Burrill et al., 2018].

Figure 1.5: Example code to produced population estimates of forest attributes grouped by discrete categories using `rFIA`.

```
## Grouping by Forest Type
biomass(db = fiaRI, grpBy = FORTYPCD)

# A tibble: 120 x 20
   YEAR FORTYPCD NETVOL_ACRE SAWVOL_ACRE BIO_AG_ACRE BIO_BG_ACRE BIO_ACRE
  <int>    <int>       <dbl>       <dbl>       <dbl>       <dbl>    <dbl>
1  2014      103       4030.       3362.        77.8        17.0     94.8
2  2014      104       3467.       2311.        74.3        16.1     90.4
3  2014      105       3876.       3403.        85.2        18.1    103.
4  2014      167       2545.       1589.        60.6        13.2     73.8
# ... with 116 more rows, and 13 more variables: CARB_AG_ACRE <dbl>,
#   CARB_BG_ACRE <dbl>, CARB_ACRE <dbl>, NETVOL_ACRE_SE <dbl>,
#   SAWVOL_ACRE_SE <dbl>, BIO_AG_ACRE_SE <dbl>, BIO_BG_ACRE_SE <dbl>,
#   BIO_ACRE_SE <dbl>, CARB_AG_ACRE_SE <dbl>, CARB_BG_ACRE_SE <dbl>,
#   CARB_ACRE_SE <dbl>, nPlots_VOL <dbl>, nPlots_AREA <dbl>
```

1.3.3.2   Unique populations of interest

In many cases, the population of interest is a subset of that represented by the full `FIA.Database`. For example, we may be interested in producing estimates for live stems greater than 12.0 inches DBH on state-owned land. Within `biomass` (and most other estimator functions), we can use the `treeDomain` and `areaDomain` arguments to describe our population of interest in terms of variables contained in the `PLOT`, `COND`, and `TREE` tables of a `FIA.Database` (Figure 1.6).

Here `treeDomain` describes the population of interest for the numerator (tree biomass) and `areaDomain` the population of interest for the denominator (state-owned forest land area). In each case, the argument takes the form of a logical predicate that is defined in terms of the variables in `PLOT`, `TREE`, and/or `COND` tables of the `FIA.Database`. Multiple conditions can be combined within either argument using `&` or `|` symbols (and/or, respectively).

Figure 1.6: Example code to produce population estimates of forest attributes within a user-defined population of interest using `rFIA`.

```
## Live tree biomass (DBH > 12") on state land
biomass(fiaRI, treeDomain = DIA > 12, areaDomain = OWNCD == 31)

# A tibble: 5 x 19
  YEAR NETVOL_ACRE SAWVOL_ACRE BIO_AG_ACRE BIO_BG_ACRE BIO_ACRE
  <int>       <dbl>       <dbl>       <dbl>       <dbl>    <dbl>
1 2014       1368.       1095.        34.8        6.96     41.7
2 2015       1396.       1094.        35.6        7.13     42.7
3 2016       1487.       1145.        38.0        7.61     45.6
4 2017       1430.       1101.        37.0        7.39     44.4
5 2018       1441.       1111.        37.3        7.45     44.7
# ... with 13 more variables: CARB_AG_ACRE <dbl>,
#   CARB_BG_ACRE <dbl>, CARB_ACRE <dbl>, NETVOL_ACRE_SE <dbl>,
#   SAWVOL_ACRE_SE <dbl>, BIO_AG_ACRE_SE <dbl>,
#   BIO_BG_ACRE_SE <dbl>, BIO_ACRE_SE <dbl>, CARB_AG_ACRE_SE <dbl>,
#   CARB_BG_ACRE_SE <dbl>, CARB_ACRE_SE <dbl>, nPlots_TREE <dbl>,
#   nPlots_AREA <dbl>
```

1.3.3.3 Grouping by user-defined areal units

To produce estimates grouped by unique areal units, specify the name of a spatial polygon object (class `sp` or `sf`) defining the areal units of interest as the `polys` argument of any `rFIA` estimator function. All FIA data are automatically re-projected to match the projection of the input spatial polygon object prior to initiating estimation procedures. All fields originally contained in the input spatial polygon object will be preserved in the estimates output by the estimator function. To return estimates as an `sf` spatial polygon object, specify `returnSpatial = TRUE`.

1.3.3.4 Alternative estimators

All `rFIA` estimator functions use the "temporally-indifferent" estimator by default (`method = "TI"`) for consistency with other FIA estimation tools, like EVALIDator [USDA Forest Service, 2019b, Pugh et al., 2018]. As an alternative, users may set the `method` argument to

Figure 1.7: Example code to produce population estimates of forest attributes for multiple values of λ using the exponential moving average estimator in `rFIA`.

```
## Most recent year in Rhode Island
## Multiple lambda values
biomass(clipFIA(fiaRI), method = "EMA" ,
        lambda = seq(from=0.1, to=0.9, by=0.1)

# A tibble: 9 x 20
  lambda  YEAR NETVOL_ACRE SAWVOL_ACRE BIO_AG_ACRE BIO_BG_ACRE
   <dbl> <int>       <dbl>       <dbl>       <dbl>       <dbl>
1    0.1  2018       2451.       1387.        68.8        13.7
2    0.2  2018       2455.       1397.        69.2        13.7
3    0.3  2018       2449.       1400.        69.2        13.7
4    0.4  2018       2432.       1393.        68.9        13.7
5    0.5  2018       2405.       1376.        68.4        13.6
# ... with 4 more rows, and 13 more variables: BIO_ACRE <dbl>,
#   CARB_AG_ACRE <dbl>, CARB_BG_ACRE <dbl>, CARB_ACRE <dbl>,
#   NETVOL_ACRE_SE <dbl>, SAWVOL_ACRE_SE <dbl>, BIO_AG_ACRE_SE <dbl>,
#   BIO_BG_ACRE_SE <dbl>, BIO_ACRE_SE <dbl>, CARB_AG_ACRE_SE <dbl>,
#   CARB_BG_ACRE_SE <dbl>, CARB_ACRE_SE <dbl>, nPlots_TREE <dbl>,
#   nPlots_AREA <dbl>
```

`"SMA"`, `"LMA"`, `"EMA"`, or `"ANNUAL"`, to use the simple moving average, linear moving average, exponential moving average, or annual estimator, respectively. If using the exponential moving average, users may also modify the exponential decay parameter, λ (Eq. 1.1), with the `lambda` argument. By default, `lambda` is set to `0.5`, although can be set to any value on the interval $(0, 1)$. If multiple values are specified as the `lambda` argument, one unique set of estimates will be returned for each unique value of `lambda` (Figure 1.7). For example, `lambda = seq(from=0.1, to=0.9, by=0.1)` will produce nine unique sets of estimates, grouped by `lambda`.

1.3.3.5   Parallelization

Parallel processing is available in all `rFIA` estimator functions using the `nCores` argument. `nCores` indicates the number of physical cores to be used and may be set to any positive

integer up to the number of physical cores available on a given machine. Serial processing is implemented by default (`nCores = 1`). Parallelization may substantially reduce memory during processing. Thus, users should consider implementing serial processing if computational resources are limited. If implementing parallel processing, we recommend users set `nCores` to one less than the number of physical cores available on their machine to ensure computational resources are available for other processes (e.g., OS, browsers).

1.4   Case study - Michigan ash decline

We demonstrate the utility of `rFIA` for forest resource monitoring by assessing the decline of ash (*Fraxinus* spp.) populations across the Lower Peninsula of Michigan following the establishment of emerald ash borer (*Agrilus planipennis Fairmaire*). Emerald ash borer is an invasive forest insect that was first discovered in southeastern Michigan in 2002. The insect spread quickly across the state and is considered one of the most destructive and costly forest insects to invade the United States [Poland and McCullough, 2006, Aukema et al., 2011]. Using the "temporally indifferent" estimator in `rFIA`, we estimated annual changes in live ash trees per acre (TPA) and tree mortality rates (mortality TPA per year) by county during the interval 2006-2018. To highlight differences among alternative design-based estimators implemented in `rFIA`, we use each estimator to assess changes in ash sawlog stocks (board feet per acre) across the entire Lower Peninsula from 2000 to 2018 and compare their relative performance (`lambda = 0.5` used for EMA estimator). All estimates were produced for white ash (*Fraxinus americana L.*), green ash (*Fraxinus pennsylvanica Marshall*), and black ash (*Fraxinus nigra Marshall*) trees ≥ 5 inches DBH.

A rapid decline of ash populations across Michigan counties is evident from our analysis. Live ash TPA decreased by 61% and annual mortality increased by 583% across the study region from 2006 to 2018 ("temporally-indifferent" estimator). Elevated mortality rates and population decline are apparent in the southeastern portion of the state soon after the establishment of emerald ash borer in the region (Figure 1.8, 2006 and 2010). In years

Figure 1.8: Changes in live ash TPA (left) and annual mortality rates (right), with associated sampling errors (bottom; 67% confidence), across counties in the Lower Peninsula of Michigan following establishment of emerald ash borer. Missing values are shaded in gray. All plots were produced using the `plotFIA` function.
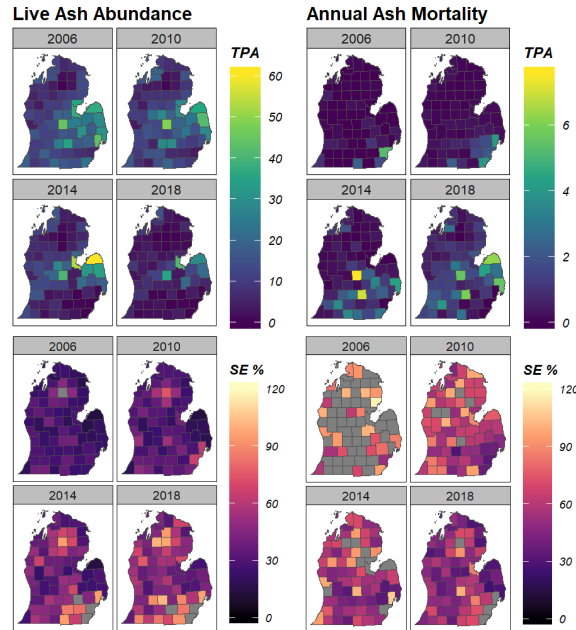
following, ash population decline and elevated mortality became evident across the Lower Peninsula, likely associated with the rapid expansion of emerald ash borer across the state (Figure 1.8, 2014 and 2018).

Sampling error is directly related to the number of non-zero observations (i.e., FIA ground plots) used to compute estimates of each variable, and cannot be determined if less than two non-zero observations are available. Decreasing precision (i.e., increased sampling errors) associated with live TPA (Figure 1.8; bottom-left) and sawlog volume (Figure 1.9; bottom) estimates indicates that the number of live ash trees located on FIA ground plots decreased over time. Ash mortality appeared to be a relatively rare event prior to the expansion of emerald ash borer across Michigan, as many counties recorded fewer than two observations of ash mortality per sampling period (gray shaded counties in bottom right of Figure 1.8). The increased frequency of ash mortality observations across Michigan counties, and associated reduction in sampling error, provides support for the trend of increased mortality rates that

Figure 1.9: Changes in ash sawlog volume (top; board feet (BF) per acre) and associated sampling errors (bottom; 67% confidence) for each design-based estimator, across the Lower Peninsula of Michigan from 2000 to 2018. All plots were produced using the `plotFIA` function.
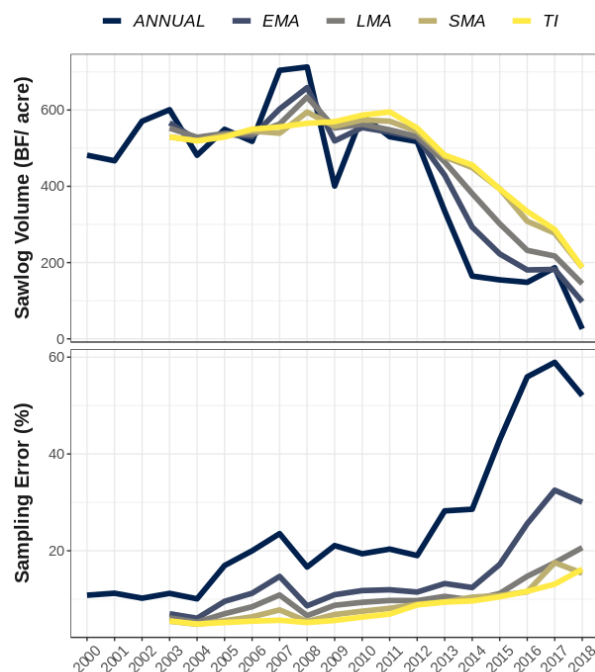
is evident following the establishment of emerald ash borer across the state.

A trade-off between temporal smoothing and precision is evident in comparing the behavior of design-based estimators implemented in `rFIA` (Figure 1.9). For example, the annual estimator (ANNUAL) appears to indicate a sharper and earlier decline (lower temporal smoothing) in the ash sawlog resource than the "temporally-indifferent" (TI) and simple moving average (SMA) estimators, though the annual estimator consistently produces higher sampling errors (lower precision) (Figure 1.9). Estimators that give more weight to recent observations, like the annual (100% of weight on most recent observation), linear moving average (LMA), and exponential moving average (EMA) tend to exhibit lower temporal lag-bias but at the cost of higher variance. In contrast, estimators that distribute weight more evenly across observations with respect to time, like the "temporally-indifferent" (no annual weighting, treated as periodic inventory) and simple moving average tend to exhibit higher

18

temporal smoothing but lower variance. In practice, we recommend users carefully consider this trade-off and choose an estimator that achieves both their desired precision standards and an acceptably low level of temporal lag-bias.

1.5   Extensions/limitations

In the future, we hope to expand `rFIA` to include model-based and model-assisted techniques, allowing users to leverage various forms of auxiliary data to improve estimation of forest attributes. Specifically, we hope to improve estimation within small domains (e.g., spatial/ temporal extents, rare forest attributes) by implementing a number of indirect and composite small area estimators. Further, we hope to improve the value of the FIA Database for detection and analysis of rapid changes in forest health through the implementation of Kalman filters as time-series estimators.

Program R is an "in-memory" application by design, and `rFIA` requires all input data to be held in RAM. Hence, users may experience memory management challenges when computational resources are limited. Memory constraints may inhibit some users from loading or processing large subsets of FIA data (relative to available computational resources), and high memory usage may result in decreased computational efficiency. Future development seeks to leverage `dplyr` [Wickham et al., 2015] back ends for external database engines such as SQLite and Apache Spark, thus reducing memory limitations and potentially offering substantial improvements in computational efficiency for large data.

Exact coordinates of FIA ground plots are not available in the public version of the FIA Database to protect privacy rights of private land owners and preserve the ecological integrity of ground plots [Tinkham et al., 2018, McRoberts et al., 2005a]. Plot locations are randomly displaced up to 1 km from their true locations (i.e., "fuzzed") and the coordinates of up to 20% of plots on private land in each county are exchanged (i.e., "swapped") [Bechtold et al., 2005, Tinkham et al., 2018]. The effects of using "fuzzed and swapped" plot coordinates are thought to be negligible for design-based estimation across large regions (800,000 acres and

larger) [McRoberts et al., 2005b], however uncertainty in true plot locations may produce results within unknown amounts of error when used in conjunction with other spatially explicit data layers for model-based estimation [Sabor et al., 2007]. Hence, we encourage `rFIA` users to consider this uncertainty when using design-based estimation for small populations, and when producing plot-level estimates to be used with spatially explicit auxiliary data in a model-based or model-assisted estimation framework.

1.6 Conclusion

The FIA database is among the most valuable ecological datasets in the world, though its complexity limits access for many potential users. We developed `rFIA` to simplify the estimation of forest attributes using FIA data, intending to provide a flexible, yet powerful toolset which is accessible to all R users. Ultimately, we hope that `rFIA` will improve the accessibility and relevance of the FIA database and promote use of FIA data among a larger, more diverse audience. We encourage users to apply `rFIA` widely and report any issues and/or desired extensions on our active issues page (https://github.com/hunter-stanke/rFIA/issues).

1.7 Acknowledgements

CHAPTER 2

OVER HALF OF TOP TREE SPECIES IN DECLINE IN THE WESTERN UNITED STATES

2.1 Introduction

Persistent shifts in forest composition, structure, and function depend largely on the demographic response of tree species to changing environmental drivers and disturbance regimes [Johnstone et al., 2016]. Many forests in the western United States (US) have experienced recent increases in the extent, severity, and frequency of wildfire [Turner et al., 2019, Stevens-Rumann et al., 2018], drought [Clark et al., 2016, Cook et al., 2004], and insect-pest outbreaks [Wong and Daniels, 2017, Bentz et al., 2010], due in part to changing climate and past forest management (i.e., fire suppression). Likewise, large-scale tree mortality events [Van Mantgem et al., 2009, Breshears et al., 2005] and recruitment failures [Davis et al., 2019, Harvey et al., 2016] indicate that widespread forest change is already underway in the region. In the face of such dramatic change, efforts to quantify the joint demographic response of tree species to anthropogenic and natural stressors are urgently needed to inform forest management and improve predictions of shifts in forest ecosystem services across the western US.

Many previous studies have quantified individual-tree demographic responses to novel stressors (e.g., global change type drought) in the western US [Van Mantgem et al., 2009, Ma et al., 2012, Py et al., 2006, Adams and Kolb, 2005, 2004], though few have examined such responses at higher levels of biological organization [Clark et al., 2016] and most only consider a single facet of tree demography. It is difficult to use knowledge inferred from trees to predict stand-level or landscape-level response to stress due to inter-tree interactions (i.e., competition, shading) [Clark et al., 2014]. Further, individual facets of tree demography (e.g., mortality, growth, recruitment) are known to interact to influence forest population

dynamics, and hence no single facet can fully explain variation in such dynamics [Franklin et al., 2002, Connell et al., 1984]. That is, increased tree mortality rates do not imply population decline if increased mortality is matched by a subsequent increase in productivity (i.e., growth, recruitment) [Assmann, 2013]. As such, a great deal of uncertainty remains regarding the current status of tree populations (e.g., expanding, declining) and how multiple drivers may interact to influence the stability of tree populations across broad spatial domains in the western US.

Multiple studies have suggested changes in the spatial distribution of tree species may be underway in the western US [Monleon and Lintz, 2015, Serra-Diaz et al., 2016, Bell et al., 2014a], driven by shifts in population dynamics (e.g., failed recruitment) at leading and trailing range margins. However, most efforts to quantify species range shifts rely on "life stage for time" substitution, wherein the potential for range shifts is measured as the magnitude of divergence between adult and juvenile tree distributions across geographic and/or bioclimatic spaces at a single point in time [Lenoir et al., 2009, Zhu et al., 2014, 2012]. Trees of each life stage established at different times and potentially under different environmental settings, and divergent distributions between tree life stages may arise from a changing environmental conditions over time. However, realized species niches often differ across tree life stages and change through the ontogeny of trees [Grubb, 1977, Miriti, 2006, Bertrand et al., 2011]. Hence it is possible that divergence in distributions across tree life stages could reflect ontogenetic differences rather than the effects of exogenous drivers (e.g., climate), and additional efforts that explicitly account for population dynamics in the estimation of species range shifts are warranted [Máliš et al., 2016].

Tree population performance (i.e., net change in abundance over time; population-level expansion, decline) emerges from the joint demographic response of individual trees to endogenous (e.g., inter-tree competition) and exogenous drivers (e.g., wildfire). Disparities in tree population performance across species, life stages, and environmental gradients may provide early indications of large-scale forest change, including species range shifts [Jackson

et al., 2009, Woodall et al., 2013, Fei et al., 2017]. For example, increased tree population performance at high elevations relative to low elevations may indicate upslope migration over time (i.e., upslope shift in abundance distribution), and inter-specific divergence in tree population performance may indicate shifts in forest composition within a region. Further, intra-specific divergence in population performance across tree life stages may predict future shifts in forest structure (i.e., shifts in abundance distribution across life stages within a region). However, comprehensive assessments of tree population performance have yet to be conducted in the western US, likely because such assessments require detailed, temporally replicated data spanning large spatial domains, which were unavailable in the region until recently [Goeking, 2015].

We sought to quantify the population performance of 10 tree species and two size classes across their ranges in the western US, and identify potential drivers of population instability (i.e., expansion or decline) where it exists. We define forest population performance in terms of shifts in abundance over time, where population stability is achieved by a balance between mortality, recruitment, and growth. That is, when mortality significantly exceeds recruitment and growth, abundance shifts downward and population decline is evident, characterized by decreased density and/or spatial extent (i.e., range contraction). In contrast, if recruitment and growth significantly exceed mortality, abundance shifts upward and population expansion occurs, characterized by increased density and/or spatial extent (i.e., range expansion). We adapt a method presented in Lintz et al. [2016] to account for transient dynamics in tree demography associated with forest structural development and succession, developing an index of forest population performance that is independent of forest composition, stand age, and ecological setting.

We draw upon over 24,000 repeated censuses of US Forest Service Forest Inventory and Analysis (FIA) plots to answer the following questions: (1) Does range-wide population performance differ among the 10 most abundant tree species in the western US, and what does spatial variation in population performance indicate about shifts in species distributions?

(2) Do tree size classes exhibit intra-specific variation in population performance, and if so, which regions experience the greatest differences? (3) How do major forest disturbances and climate influence the population performance of tree species and size classes, and what do these relationships suggest about the drivers of species decline where it exists?

2.2   Materials and Methods

2.2.1   Field observations

Since 1999, the FIA program has operated an extensive, nationally-consistent forest inventory designed to monitor changes in forests across all lands in US [USDA Forest Service, 2019a]. We used FIA data from 10 states in the western US (Washington, Oregon, California, Idaho, Montanta, Utah, Nevada, Colorodo, Arizona, and New Mexico) to quantify forest population performance, excluding Wyoming due to a lack of repeated censuses. This region spans a wide variety of climatic regimes and forest types, ranging from temperate rain forests of the coastal Pacific Northwest to pinyon-juniper woodlands of the interior southwest [Eyre, 1980]. Although the spatial extent of the FIA plot network represents a large portion of the current range of all species examined in this study, substantial portions of some species ranges (e.g., western hemlock) extend beyond the study region into Canada and/or Mexico and therefore were not fully addressed here.

The FIA program measures forest attributes on a network of permanent ground plots that are systematically distributed at a rate of approximately 1 plot per 2500 hectares across the US [Smith, 2002]. For trees $12.7cm$ diameter at breast height (DBH) and larger, attributes (e.g., species, DBH, live/dead, mortality agent) are measured on a cluster of four $168m^2$ subplots [Bechtold et al., 2005]. Trees $2.54 - 12.7cm$ DBH are measured on a a microplot $(13.5m^2)$ contained within each subplot, and rare events such as very large trees are measured on an optional macroplot $(1012m^2)$ surrounding each subplot [Bechtold et al., 2005]. In the western US, one-tenth of ground plots are measured each year, with re-measurements first occurring in 2011.

We characterized forest disturbance severity at each remeasured FIA plot as the annual fraction of mortality, in terms of tree basal area per unit area (BAA), attributed by FIA field crews to one of four mortality agents during the re-measurement interval: fire, insects, disease, and harvest/ landclearing. Specifically, we estimate disturbance severity for each mortality agent as:

$$d_j = \frac{2}{r} \frac{BAA_{mort,j}}{BAA_{2,live} + BAA_{1,live}} \tag{2.1}$$

where d_j is disturbance severity for mortality agent j, $BAA_{mort,j}$ is the the total BAA killed by mortality agent j during the re-measurement interval r (including stems that recruited and subsequently died within the measurement interval), and $BAA_{1,live}$ and $BAA_{2,live}$ is the total live BAA at initial and final measurements, respectively. Hence, we represent annual change in BAA due to each mortality agent with respect to the average live BAA between measurements, yielding a symmetric index of change that accommodates initial measurement equal of (i.e., no trees present at initial measurement) [Törnqvist et al., 1985].

2.2.2 Climate data

We acquired 30 year precipitation and mean temperature normals from the 4-km resolution PRISM climate dataset [PRISM Climate Group, 2010] and extracted data for each FIA plot location to generate long-term climate variables. While forests may respond to variation in climate at relatively fine spatial scales [Millar et al., 2018, Case and Peterson, 2005], particularly in regions with complex topography, coarse resolution climate data are often adequate to characterize broad-scale climatic controls on forest processes [Ashcroft, 2010, Pearson and Dawson, 2003], such as those addressed here. Furthermore, our ability to account for fine scale climatic microrefugia that may not be represented by broad scale climate data was limited by precision in FIA plot locations, which are randomly displaced

up to 1 km from their true locations to protect privacy rights of private land owners [Tinkham et al., 2018].

We used the Standardized Precipitation Evapotransporitive Index (SPEI) to characterize drought severity between repeated measurements on each FIA plot. The SPEI is a multi-scalar drought index widely used for assessing the impacts of drought on forests and other terrestrial ecosystems [Wu et al., 2018, Vicente-Serrano et al., 2013, Jiang et al., 2019, Huang et al., 2015, Greenwood et al., 2017]. The SPEI has advantages over other drought indices (e.g., Palmer Drought Severity Index) as it allows direct comparison of drought severity across geographic space and can be used to identify drought on a variety of time-scales [Vicente-Serrano et al., 2010]. We computed the SPEI using 4-km monthly precipitation and mean temperature estimates from the PRISM climate dataset [PRISM Climate Group, 2010]. Specifically, we computed the SPEI on a monthly basis with an 18 month time-lag for the period 1999-2018 using the SPEI R package [Beguería et al., 2014, Beguería and Vicente-Serrano, 2017], estimating potential evapotranspiration using the Thornthwaite method [Thornthwaite, 1948]. We chose to compute the SPEI with an 18 month time lag as many forest processes (i.e., mortality, growth) commonly exhibit lagged responses to drought, ranging from months to several years [Vanoni et al., 2016, Bigler et al., 2007, Klockow et al., 2018, Clark et al., 2016]. We defined drought severity at each FIA plot as the mean monthly SPEI experienced at each location during the re-measurement interval.

2.2.3 Forest stability index

We adapt a method developed by Lintz et al. [2016] to produce an index of forest population performance for each remeasured FIA plot. We first estimate annual rate of change in live trees per unit area (ΔTPA) and live basal area per unit area (ΔBAA) as change in each variable between measurements divided by the re-measurement interval on each plot. We then scale each rate of change by dividing by the respective sample standard deviation:

Figure 2.1: Example relationship of change in TPA (S, x-axis) and change in BAA (B, y-axis) for subalpine fir (*Abies lasiocarpa*) in Colorado (all plots remeasured from 2015-2018). Small diameter circles represent plot level-indices of S and B, and the single large diamond represents the region-wide mean for each dimension. Small squares distributed on the 1:1 line (gray-dashed line) represent plot-level FSI values corresponding to six example plots in the upper-right of the graph (connected by by black segments). All points are colored by their respective FSI value. Points in the bottom-left of the graph are characterized by losses in both TPA and BAA, indicating the species is likely declining within these stands. Conversely, points in the upper-right of the graph are characterized by increases in TPA and BAA, indicating species is likely expanding in the stand (i.e., increasing in density).
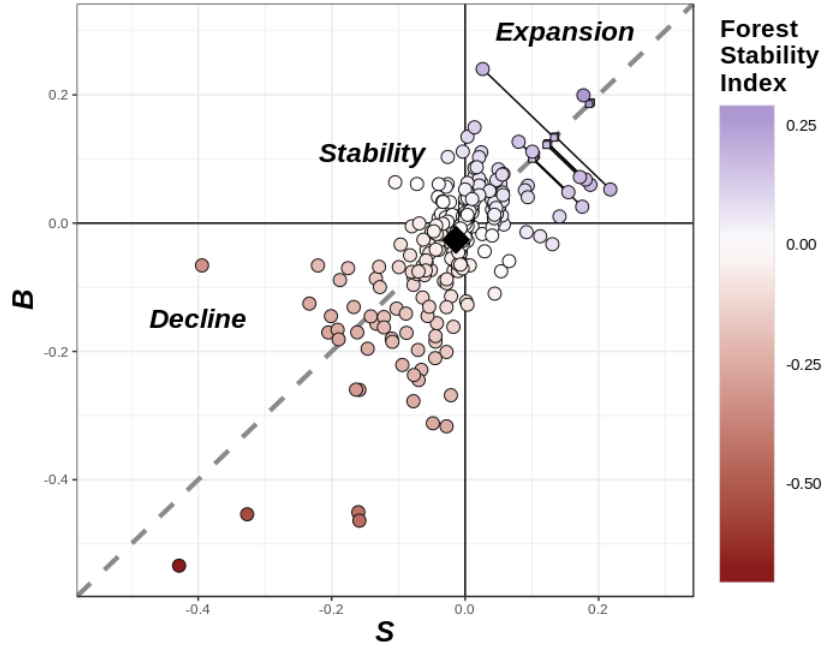
$$S_i = \frac{\Delta TPA_i}{sd(\Delta TPA)} \tag{2.2}$$

$$B_i = \frac{\Delta BAA_i}{sd(\Delta BAA)} \tag{2.3}$$

where B_i is scaled annual change in BAA on plot i, S_i is scaled annual change in TPA on plot i, and $sd(x)$ denotes the standard deviation of variable x. We represent change on a unit area basis to account for differences in sampling areas between tree size classes. We use the sample standard deviation to scale ΔTPA and ΔBAA so that each rate has equal variance ($\sigma = 1$), and hence one unit change in S is equivalent in magnitude to one unit

change in B.

We project plot-level S and B perpendicularly onto the 1:1 line to produce a single metric of population performance, herein referred to as the Forest Stability Index (FSI) (Figure 2.1; small squares). Reducing S and B to a single dimension (i.e., the FSI) facilitates summary across geographic, temporal, and bioclimatic spaces, and simplifies interpretation of the direction and magnitude of population change. Summarized across a large sample of plots (i.e., a meta-population), the FSI supports the following premise: if net changes in BAA and TPA are significantly greater than 0 (Figure 2.1, top-right), the underlying population is likely expanding in the region (i.e., increasing in density and/or spatial extent). Conversely, if net changes in BAA and TPA are significantly less than 0 (Figure 2.1, bottom-left), population decline is likely and further examination to identify potential drivers is warranted. Finally, if net changes in BAA and TPA are not significantly different from zero (Figure 2.1, center), change in the underlying population is negligible (i.e., the population is stable).

Standardized changes in TPA (S) and BAA (B) may be directly compared among species and across site conditions under the premise that mortality, recruitment, and growth rates, which implicitly define S and B, will be balanced for any stable population (i.e., net change of zero). Inherent differences among species life-history traits (e.g., shade tolerance) and spatial variation in resource availability (e.g., light, moisture, nutrients) maintain a demographic trade-off between tree growth and mortality rates [Assmann, 2013, Wright et al., 2004, Grubb, 1977, Pacala et al., 1996]. That is, variation in mortality rates are offset by variation in growth rates across species and site conditions, with fast-growing species and high productivity sites tending to experience higher mortality rates than slow-growing species and low productivity sites.

Independently, S and B are confounded by transient dynamics associated with stand structural development and succession, however we argue that these dynamics are offsetting when both indices are considered simultaneously using the FSI. For example, mortality in young forests may exceed recruitment due to inter-tree competition (negative S), albeit this

loss is offset by growth on surviving trees (neutral or positive B) and is therefore sustainable (Figure 2.1, top-left) [Franklin et al., 2002]. Furthermore, mortality of individual large trees is likely to exceed recruitment and growth among surviving stems when measured in terms of basal area in old forest (negative B), where basal area is often distributed disproportionately among large trees [Parobeková et al., 2018]. However in the same scenario, mortality may be far exceeded by recruitment in terms of trees per acre, as the loss of an individual large tree may coincide with recruitment of many young trees (positive S) (Figure 2.1, bottom-right).

2.2.4 Statistical analysis

We computed the FSI by species and by tree size class for all remeasured FIA plots in the western US ($N = 24,229$). We included plots on both public and private lands and included all live stems ($DBH \geq 1$ inch). All plot measurements included in our analysis occurred from 2001-2018, with an average re-measurement interval of 9.78 years ($\pm$ 0.005 years). For brevity, we restricted our analysis to consider the 10 most abundant tree species in the western US and simplified tree size classifications to include two classes: small diameter (2.54-12.6 cm DBH) and large diameter (DBH ≥ 12.7 cm). We identified the most abundant tree species across our study area using the `rFIA` R package [Stanke et al., 2020], defining abundance in terms of estimated total number of trees (DBH ≥ 2.54 cm) in the year 2018. We excluded species that exhibit non-tree (i.e., shrub, subshrub) growth habits across portions of the study region (e.g., *Quercus gambelii*).

We applied stratified random estimators described by the FIA program [Bechtold et al., 2005] to estimate the range-wide mean and variance of the FSI for each population defined by species and tree size class. Specifically, we used the simple moving average estimator implemented in the `rFIA` R package [Stanke et al., 2020] to compute estimates from a series of eight annual panels (i.e., sets of plots re-measured in the same year) ranging from 2011-2018. The simple moving average estimator combines information from annual panels with equal weight (i.e., irrespective of time since re-measurement), thereby allowing us to characterize

long-term patterns in population performance. We determine populations to be stable if the 95% confidence intervals for estimated range-wide FSI included zero. Alternatively, if confidence intervals of estimated range-wide FSI do not include zero, we determine the population to be expanding when the FSI is positive and declining when the FSI is negative.

We assessed geographic variation in species population performance, independent of tree size class, by estimating the FSI for each species within ecoregion subsections [Moore et al., 2016] using the simple moving average estimator. As a direct measure of changes in abundance, spatial variation in the FSI is indicative of spatial shifts in species distributions during the re-measurement interval (i.e., range expansion/contraction and/or within-range abundance shifts). That is, the distribution of any population shifts towards regions of high population performance and away from regions of low population performance during the temporal frame of sampling. We map estimates of the FSI for each ecoregion subsection to assess spatial patterns in species population performance across their range and identify regions where widespread geographic shifts in species distributions may be underway.

We determined if range-wide population performance of individual species diverged significantly between tree size classes by applying Kruskall-Wallis tests to plot-level FSI values grouped by species and size class. We assessed geographic variation in this intra-specific divergence in population performance by applying Kruskal-Wallis tests to the same plot-level FSI values within each ecoregion subsection. Hence for each species, we assessed if mean FSI values differed significantly between tree size classes within each ecoregion subsection included in its range. We then map significant differences to assess spatial patterns of divergence in species population performance between tree size classes.

We sought to determine the relative importance of forest disturbance processes and long-term climate patterns (Figure 2.2) in shaping the population performance of species and tree size classes across our study region. We used linear mixed-effects models to predict plot-level FSI as a function of forest disturbance severity rates (i.e., insects, fire, disease, harvest/landclearing, and drought) and long-term climate normals (i.e., precipitation and

Figure 2.2: Spatial variation in forest disturbance severity and long-term climate patterns across the study region. All variables standardized to a common scale for visual interpretation of spatial variation.
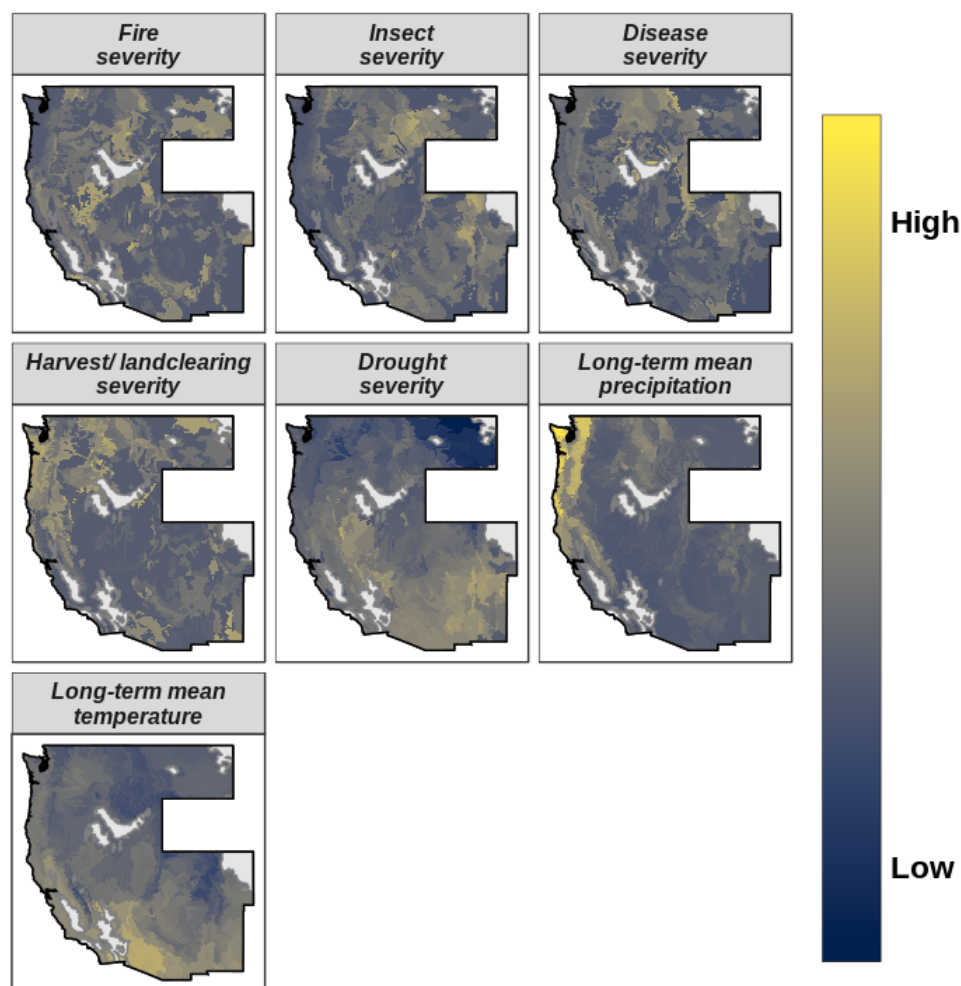
mean temperature). We included species and tree size as random effects and allowed slopes of each predictor to vary across groups. We ensured minimal collinearity between predictor variables using variance inflation factors. We standardized all predictors at the species level prior to analysis, and compared coefficients estimated by the model to interpret the relative importance each predictor in explaining variation in the FSI.

2.3 Results

We sought to quantify the population performance of the 10 most abundant tree species across their ranges in the Western US, and identify drivers of instability where it exists.

Table 2.1: Scientific and common names of ten most abundant species across our study area, listed in order of increasing abundance (i.e., bottom being most abundant; abundance defined by estimated total number of trees). Sample size (number of re-measured FIA plots where the species occured) provided for small diameter (2.54-12.6 cm DBH), large diameter (DBH $\geq$ 12.7 cm DBH), and combined populations (DBH $\geq$ 2.54 cm). As large diameter and small diameter populations of a species may exist on the same plot, the sample size of the combined population is not equal to the sum of large diameter and small diameter sample sizes.

| | | Number of plots | | |
Common name	Scientific Name	Large diameter	Small diameter	Combined
Western hemlock	*Tsuga heterophylla*	3149	1617	3262
Grand fir	*Abies grandis*	2580	1439	2734
Utah juniper	*Juniperus osteosperma*	3425	891	3446
Engelmann spruce	*Picea Engelmannii*	2965	1287	3079
Quaking aspen	*Populus tremuloides*	1563	935	1723
Common pinyon	*Pinus edulis*	2998	1423	3076
Ponderosa pine	*Pinus ponderosa*	7177	2352	7309
Subalpine fir	*Abies lasiocarpa*	3003	1964	3174
Lodgepole pine	*Pinus contorta*	4388	2276	4556
Douglas-fir	*Pseudotsuga menziesii*	12086	4688	12284

We identified the 10 most abundant tree species by their estimated total number of stems, including 7 distinct genera and 3 families (Table 2.1). Together these top 10 species accounted for 68.9% of all trees across the study region (64.4% of total basal area) (Figure 2.3). As expected, small diameter stems were more abundant than large diameter stems for most species in terms of tree number. The relative abundance distributions provided in Figure 2.3 are intended to aid in interpretation of assessments of population performance that follow, providing a reference upon which we can base assessments of population change.

Differences in range-wide mean FSI illustrate substantial variation in population performance among species. Irrespective of tree size class, we found 70% of species populations in decline and the remaining 30% expanding across the study region (Figure 2.4, left). The highest rates of decline appeared in Engelmann spruce and subalpine fir populations, characteristic species of moist, high-elevation regions of the Rocky Mountains. In contrast, we observed the highest rates of population expansion in grand fir and western hemlock, which

Figure 2.3: Region-wide prevalence (% of total tree population across the study region) of the 10 most abundant tree species in the western US in 2018. Estimates provided for combined (left), large diameter (center), and small diameter populations (right). Species listed in order of increasing abundance with respect to the combined population (i.e., bottom being most abundant).
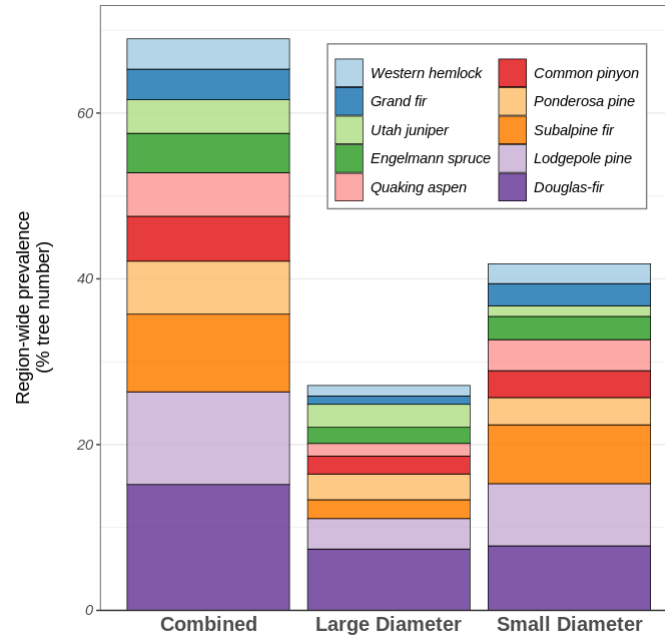
occur predominantly in low-mid elevation forests of the Pacific Northwest (i.e., Washington, Oregon, Idaho, and western Montana).

Qualitatively, we observed considerable variation in the spatial patterns of population performance among species (Figure 2.5 (Top)). Populations of Engelmann spruce, Douglas-fir, and ponderosa pine appear to be generally expanding in the Pacific Northwest and Sierra Nevadas, while subalpine fir and lodgepole pine are generally declining in the region. Grand fir and western hemlock appear to be expanding predominantly in the Northern Rockies and Interior Pacific Northwest, and declining in the coastal Pacific Northwest. Widespread decline of lodgepole pine is evident in the Central Rocky Mountains, while no clear pattern emerges for Douglas-fir, ponderosa pine, Engelmann spruce, and subalpine fir in the region (i.e., both expansion and decline occur frequently). Decline appears to be wide-spread among Engelmann spruce, subalpine fir, and ponderosa pine in the Sourthern Rocky Mountains. Quaking aspen populations generally appear to be in decline in the southern portions of its

Figure 2.4: Range-wide mean Forest Stability Index (FSI) of the 10 most abundant tree species in the western US. Estimates provided for combined (left), large diameter (center), and small diameter populations (right). Population decline (red) occurs when the FSI is negative and the associated confidence interval does not include zero. Conversely, population expansion (blue) occurs when the FSI is positive and the associated confidence interval does not include zero.
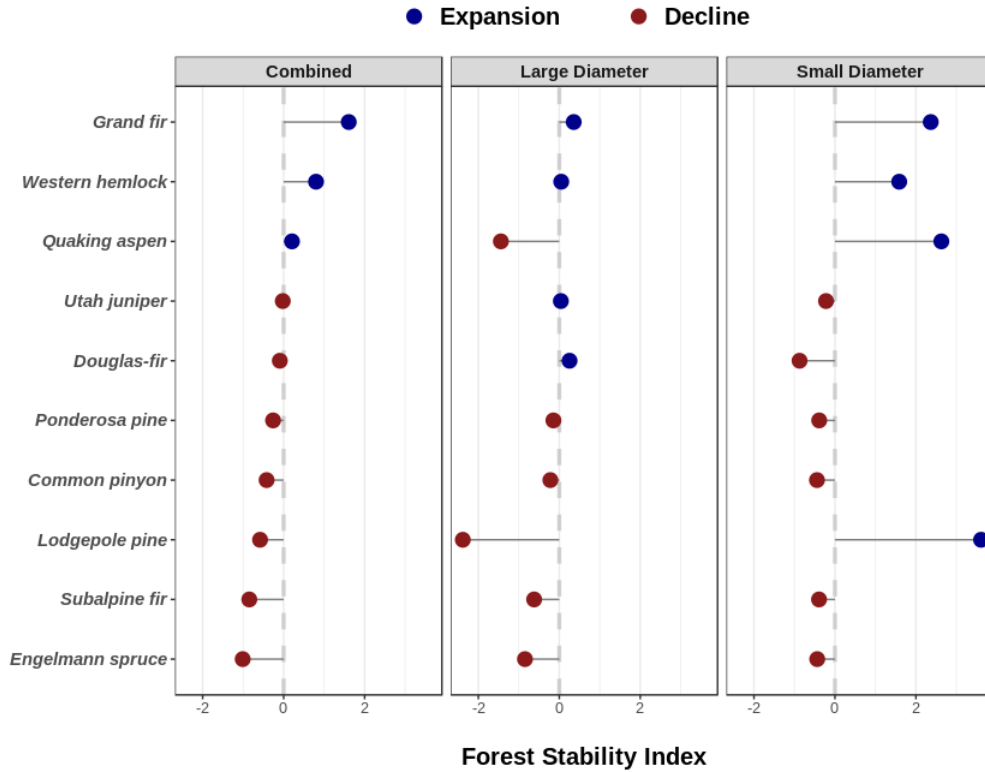
range (Southern Rocky Mountains) and expanding in the northern portions (Northern Rocky Mountains, Interior Pacific Northwest). It appears Utah juniper tends to be declining near the spatial margins of its range (i.e., decline appears more frequently in outermost areas of its range) and expanding in the central portion of its range. The opposite pattern appears for common pinyon, with expansion prevalent near the spatial margins of its range and decline prevalent in the central portion.

We found evidence of intra-specific divergence in range-wide population performance between tree size classes for 80% of species (Figure 2.4, Large Diameter vs. Small Diameter). Specifically, we found significant differences ($P \leq 0.05$) in mean FSI between small diameter and large diameter populations for all species except Utah juniper and Engelmann spruce

Figure 2.5: (Top) Spatial variation in population performance of species across their ranges. Forest Stability Index (FSI) summarized within ecoregion subsections using the simple moving average estimator. Population expansion occurs if the mean FSI significantly exceeds zero within an area (net increase in abundance), and population decline occurs if the mean FSI is significantly less than zero (net decrease in abundance). Populations are determined to be stable within an area if the confidence interval of estimated mean FSI includes zero. (Bottom) Spatial variation in intra-specific differences in population performance between tree size classes. Areas where small diameter populations exhibit significantly higher FSI than large diameter populations shaded in purple. Conversely, areas where small diameter populations exhibit significantly lower FSI than large diameter populations shaded in yellow. Otherwise populations are determined to be changing at equal rates (green).
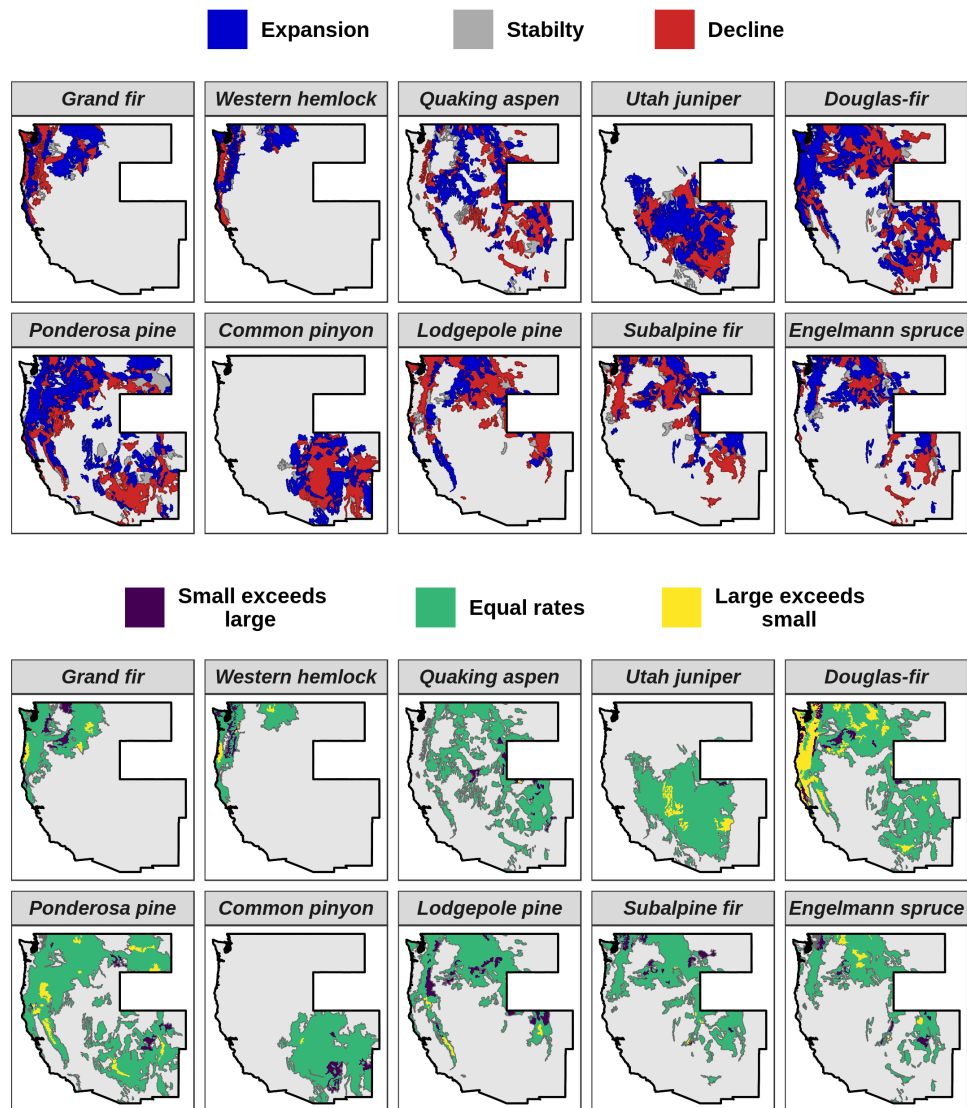
Table 2.2: Intra-specific differences in range-wide mean Forest Stability Index (FSI) between tree size classes. Significance (i.e., p-values) derived from Kruskall-Wallace test using plot-level FSI values.

	FSI ± 95% CI			
Species	Large diameter	Small diameter	Difference	P Value
Grand fir	0.36 ± 0.004	2.36 ± 0.020	-2.00	≤ 0.001
Western hemlock	0.05 ± 0.004	1.58 ± 0.024	-1.53	≤ 0.001
Quaking aspen	-1.44 ± 0.002	2.63 ± 0.020	-4.07	≤ 0.001
Utah juniper	0.04 ± 0.001	-0.22 ± 0.004	0.26	0.413
Douglas-fir	0.25 ± 0.001	-0.87 ± 0.004	1.12	≤ 0.001
Ponderosa pine	-0.15 ± 0.001	-0.39 ± 0.008	0.24	≤ 0.001
Common pinyon	-0.22 ± 0.001	-0.44 ± 0.006	0.22	0.014
Lodgepole pine	-2.38 ± 0.003	3.61 ± 0.020	-5.99	≤ 0.001
Subalpine fir	-0.62 ± 0.002	-0.39 ± 0.008	-0.23	≤ 0.001
Engelmann spruce	-0.85 ± 0.002	-0.44 ± 0.005	-0.41	0.281

(Table 2.2). The FSI of small diameter populations significantly exceeded that of large diameter populations of grand fir, western hemlock, quaking aspen, lodgepole pine, and subalpine fir. In contrast, the FSI of large diameter populations significantly exceeded that of small diameter populations of Douglas-fir, ponderosa pine, and common pinyon.

We used Kruskall-Wallace tests to identify regions (i.e., ecoregion subsections) with significant intra-specific differences in mean population performance between tree size classes. We found no significant divergence in population performance across the majority of each species range (2.5 (bottom); Equal rates), however general spatial patterns of divergence do appear for some species. Specifically, the FSI of large diameter Douglas-fir populations exceeds that of small diameter populations frequently in the coastal Pacific Northwest. Other areas where the FSI of large diameter populations exceeds that of small diameter populations were observed sporadically across the ranges of Douglas-fir, Utah juniper, western hemlock, grand fir, ponderosa pine, lodgepole pine, and Engelmann spruce. The opposite, where the FSI of small diameter populations exceeds that of large diameter populations, was observed sporadically across the ranges of all species except Utah juniper.

Results of our linear mixed model reveal that forest disturbance processes are generally

Figure 2.6: Standardized coefficients of the linear mixed-effect model predicting plot-level FSI as a function of forest disturbance severity and long-term climate patterns. All variables were scaled at the species level, hence the relative importance of each predictor in explaining intra-specific variation in population performance may be directly inferred from the magnitude of each coefficient. That is, coefficient values can be directly compared across tree size classes (i.e., vertically) but not across species (i.e., horizontally). Blue shaded backgrounds indicate the population is expanding across the study region (e.g., large diameter grand fir; top left). Red shaded backgrounds indicate the population is declining across the study region (e.g., large diameter Engelmann spruce; top right). Error bars represent the 95% confidence intervals in the estimate of each coefficient.
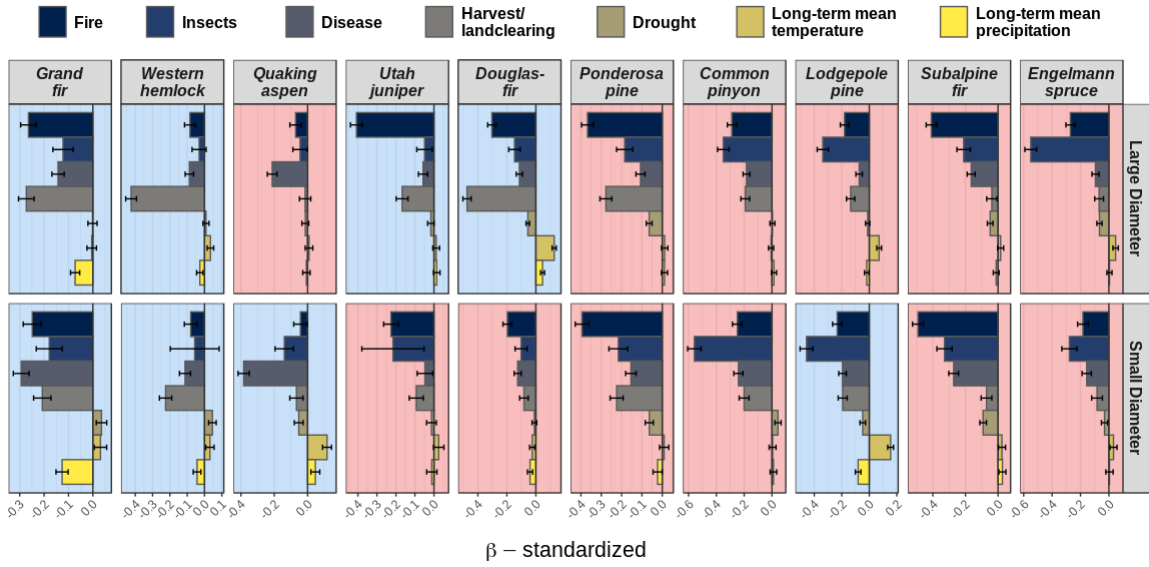
much more important than long-term climate patterns in shaping the population performance of species and tree size classes (Figure 2.6). We found a negative relationship between the FSI and all forest disturbance severity variables except drought, which exhibited both positive and negative relationships with the FSI dependent upon species and tree size class. That is, increases in severity of all forest disturbances, with the exception of drought, coincided with decreased FSI values (i.e., higher rates of decline or lower rates of expansion) for all species and tree size classes. In contrast, we found that long-term climate variables (i.e., long-term precipitation and mean temperature) vary considerably in their relationship to the FSI across species and tree size classes.

Among large diameter stems, we found fire severity was among the two most important predictors of the FSI for all species except western hemlock (Figure 2.6). We found harvest/

landclearing to be of high importance (i.e., top two predictors) for large diameter grand fir, western hemlock, Douglas-fir, Utah juniper, and ponderosa pine, all of which except ponderosa pine exhibited range-wide expansion. Insect outbreak severity was of high relative importance for large diameter common pinyon, lodgepole pine, subalpine fir, and Engelmann spruce, all of which we determined to be undergoing range-wide population decline. We found disease severity to be the most important predictor of large diameter quaking aspen FSI, but less important for all other species. We found drought to be among the least important forest disturbance processes associated with large diameter population performance across all species.

We found the relative importance of forest disturbance processes in relation to the population performance to be similar for each species across size classes, although some notable differences did appear (Figure 2.6). We found that insect outbreak severity was substantially more important in predicting the FSI of small diameter populations of all species except western hemlock, Douglas-fir, and Engelmann spruce, where Engelmann spruce exhibited the opposite relationship (i.e., insect outbreak more important for large-diameter than small diameter). Similarly, we found that disease severity was substantially more important in predicting the FSI of small diameter populations of grand fir, quaking aspen, ponderosa pine, lodgepole pine, subalpine fir, relative to that of large diameter populations of the same species. We found the importance of harvest/ landclearing to be markedly lower in small diameter populations of species for which it was identified as an important predictor of FSI in large diameter populations. Finally, we found drought to be a more important predictor of small diameter populations of all species except ponderosa pine, Utah juniper, Douglas-fir, and Engelmann spruce, where Douglas-fir and Engelmann spruce exhibited the opposite relationship.

While generally less important than disturbance processes, we found significant relationships between long-term climate variables and population performance for multiple species and tree size classes. The FSI of large and small diameter populations of grand fir and

western hemlock, as well as populations of small diameter Douglas-fir and lodgepole pine, exhibited significant negative relationships with long-term mean precipitation, indicating improved population performance in dry regions. We observed the opposite relationship in large diameter Douglas-fir and small diameter quaking aspen (i.e., improved population performance in wet regions). Further, we observed significant positive relationships between the FSI and large diameter populations of western hemlock, Douglas-fir, and Engelmann spruce, as well as small diameter populations of quaking aspen and lodgepole pine, indicating improved population performance in warm regions. Neither large and small diameter populations of Utah juniper, ponderosa pine, common pinyon, and subalpine fir exhibited a significant relationship with long-term climate variables.

2.4 Discussion

2.4.1 Range-wide population performance and regional shifts in forest composition

Our results indicate a majority (7 of 10) of the most abundant tree species in the western US are undergoing significant range-wide population decline (Figure 2.4). This result coincides with recent reports of widespread tree mortality across the region [Van Mantgem et al., 2009, Breshears et al., 2005, Bigler et al., 2007, Lintz et al., 2016], suggesting that heightened tree mortality is likely driving forest decline in the western US. However, our results indicate that population performance varies considerably between species, and that some species (grand fir, western hemlock, and quaking aspen) are experiencing significant range-wide population expansion. Such dramatic divergence in range-wide population performance between tree species may provide early indications of broad-scale shifts in forest composition across the western US, where high performing species increase in abundance relative to lower performing species.

We observed the highest rates of range-wide population decline in Engelmann spruce, subalpine fir, and lodgepole pine, all of which tend to occur at high-elevation near the upper

forest ecotone across the western US [Peet, 1981]. Combined, these species represent 25.3% of all trees across the region (Figure 2.3). Previous efforts have indicated that subalpine tree species are among the most vulnerable to future changes in climate and forest disturbance regimes [Bell et al., 2014b, Conlisk et al., 2017, Wong and Daniels, 2017, Bigler et al., 2007, Malone et al., 2018]. Our results indicate this heightened vulnerability may already be manifesting across the western US, serving as an early warning sign of widespread, pervasive decline of subalpine forests.

In contrast, we observed the highest rates of range-wide population expansion in grand fir and western hemlock (Figure 2.4), together representing 7.3% of all trees across the western US. Both grand fir and western hemlock are extremely shade tolerant, late seral species occurring predominately on cool, mesic sites in the northern portion of our study region [Burns, 1990, Peet, 1981]. Population expansion of shade tolerant species is consistent with compositional shifts expected under accelerated secondary succession [Franklin et al., 2002]. Across the dry domain of the western US, decades of fire exclusion and selective harvesting have created crowded, light-competitive stand conditions that favor the expansion of shade tolerant tree species [Hessburg et al., 2005, Hessburg and Agee, 2003, Naficy et al., 2010, Gallant et al., 2003]. Hence, we argue the population expansion of grand fir and western hemlock emerges as an artifact of past forest management (i.e., fire suppression, selective silvicultural systems), and presents a prominent challenge for contemporary dry forest restoration.

We found population performance was most stable among characteristically montane (i.e., Douglas-fir, ponderosa pine, quaking aspen) and woodland species (i.e., Utah juniper, common pinyon) in the western US, indicated by FSI values closest to zero. Significant range-wide decline was evident in all such species except quaking aspen, which was determined to be expanding slightly across its range (Figure 2.4). Our results concur with those presented by Lintz et al. [2016], who reported higher levels of density-independent mortality in subalpine species relative to montane and woodland species. It is important to note that the high

frequency of decline among montane and woodland species, albeit marginal, may not be undesirable if management objectives aim to reduce overall tree density, thereby promoting stand structure more similar to that of pre-suppression eras.

2.4.2   Forest disturbances as drivers of tree population performance

We found insect outbreaks and wildfire to be the most important drivers of population decline in subalpine tree species (Engelmann spruce, subalpine fir, and lodgepole pine), although disease was also important for subalpine fir (Figure 2.6). This result is consistent with previous findings that indicate elevated mortality in lodgepole pine, Engelmann spruce, and subalpine fir are linked closely with outbreaks of mountain pine beetle (*Dendroctonus ponderosae*) [Page and Jenkins, 2007], spruce beetle (*Dendroctonus rufipennis*) [DeRose and Long, 2012], and subalpine fir decline (i.e., a complex disorder caused by multiple mortality agents) [Reich et al., 2016], respectively. Furthermore, increased frequency and extent of severe fire [Turner et al., 2019] and post-fire drought [Harvey et al., 2016] have been linked to recruitment declines in subalpine forests across the region. Future shifts in forest disturbance regimes [Buma et al., 2013, Turner et al., 2019], paired with expected declines in climate suitability [Dobrowski et al., 2015, Bell et al., 2014b], suggest the future of subalpine tree species in the western US may be grim.

Though the effects are marginal, we found that population performance of small diameter grand fir and western hemlock exhibited positive response to drought severity (Figure 2.6), supporting a narrative of dry-site encroachment by these species. That is, performance of small diameter populations increases with increasing drought severity, potentially driven by increased light and/or moisture availability arising from heightened mortality of large diameter trees that are more susceptible to drought [Bennett et al., 2015, Stovall et al., 2019]. We found other forest disturbances to be more important than drought in explaining variation in population performance of grand fir and western hemlock. However the most important drivers varied substantially between the species, potentially indicating the species

have fundamentally different exposures to forest disturbances.

Among montane and woodland species, we found wildfire and insect outbreaks to be among the most important drivers of population performance, though disease exhibited strong control on quaking aspen performance, as expected given widespread dieback of the species due to sudden aspen decline [Worrall et al., 2010, Marchetti et al., 2011, Rehfeldt et al., 2009]. As expected for important commercial timber species, we found that harvest and landclearing was also an important driver for Douglas-fir and ponderosa pine. In general, the importance of major forest disturbances was similar between subalpine and montane species, however higher rates of decline among subalpine species may further highlight that these species are more vulnerable to shifts in forest disturbance patterns.

2.4.3   Early indications of species range shifts

Future shifts in tree species distributions in response to changes in climate and forest disturbance regimes are widely expected [Davis and Shaw, 2001, Allen et al., 2010, Iverson et al., 2008]. Previous efforts to detect such shifts have compared the distribution of tree life stages at a single point in time (i.e., life stage for time substitution), but we present one of the first to directly incorporate temporally replicated observations of species abundance across the western US. We observed variation in population performance across the ranges of all species (Figure 2.5), indicating that significant geographic shifts in species abundance distributions have occurred over the last two decades. However, we found that the spatial pattern of species abundance shifts were far more complex than the higher latitudinal–elevation fingerprint generally expected under climate change. The complexity of species abundance shifts observed in this study are consistent with findings of previous works in the region [Bell et al., 2014b, Serra-Diaz et al., 2016, 2015, Dobrowski et al., 2015], which attribute such complexity to interactions among climate patterns, topography, and biotic drivers (i.e., competition, succession).

While generally less important than forest disturbances, we found significant relationships

between population performance and long-term climate variables for some tree species (Figure 2.6), indicating that significant shifts in species abundance distributions have occurred across climatic gradients. Most notably, we observed a positive association between tree population performance and long-term mean temperature for all species/ size class pairs where a significant relationship between the variables existed, indicating a shift in abundance toward historically warmer regions. This result counters the expectation of upslope migration expected under globally warming temperatures, and indicates that shifts in species abundances may be driven instead by transient downslope migration mediated by biotic interactions, as noted in Lenoir et al. [2009]. Relationships were more nuanced between population performance of species/ size class pairs and long-term precipitation patterns. However, grand fir population performance exhibited a strong, negative association with long-term precipitation (i.e., population performance enhanced on historically dry sites), providing additional support for the narrative of dry-site encroachment by the species.

2.4.4 Intra-specific divergence in population performance among size classes

Variation in population performance across tree size classes can have important ramifications for forest structure. That is, population expansion among small diameter stems of a species may offset population decline among large diameter stems, resulting in similar forest composition, but substantial shift in abundance towards small diameter stems over time [Dolanc et al., 2013]. We observe significant divergence in range-wide population performance between tree size classes for most species (80%), though the magnitude and direction of divergence varied both by species (Table 2.2) and across space (Figure 2.5; bottom). The largest divergence appeared in quaking aspen and lodgepole pine, where we observed severe decline was evident among large diameter stems and rapid expansion among small diameter stems. Both quaking aspen and lodgepole pine have experienced recently elevated rates of mortality due to sudden aspen decline [Worrall et al., 2010, Marchetti et al., 2011] and mountain pine beetle [Page and Jenkins, 2007], respectively, and it is likely that these agents

43

contributed to the decline of large diameter populations of each species. However, population expansion observed in small diameter stems could be attributed to increased regeneration rates in response to elevated mortality levels (i.e., increased resource availability) within each species current distribution, an expansion of each species range beyond its current distribution (i.e., driven by increased regeneration rates at range margins), or a combination of both. Further efforts to identify the drivers of such intra-specific divergence in population performance across tree size classes are warranted.

2.5 Conclusions

In recent decades, forests of the western US have experienced unprecedented change in climate and forest disturbance regimes, and widespread future shifts in forest composition, structure, and function are expected in response [Williams et al., 2013, Dobrowski et al., 2015, Liu et al., 2013]. However, large-scale, comprehensive assessments of tree population performance have yet to be conducted in the region, and uncertainty remains regarding the current status of tree populations (e.g., expanding, declining) and how multiple drivers may interact to influence their stability. Our study provides empirical evidence to suggest the most abundant tree species in the western US are exhibiting strong divergence in population performance, with over half (70%) of species experiencing range-wide population decline. We found spatial variation in population performance across the ranges of all species, indicating range shifts are already underway and are pervasive among top species in the region. Our results further indicate that species decline can seldom be attributed to a single forest disturbance agent, highlighting the importance of considering multiple, simultaneous risks factors when interpreting forest decline.

APPENDIX

APPENDIX

APPENDIX A

This appendix is intended to serve as further reference to section 2.3, Software Testing. We have conducted extensive validation of `rFIA` for all available attributes against EVALIDator. Here we present the code used to produce an abbreviated version of a validation for the state of Connecticut in the year 2018 (Table 1, section 2.3). First we download the state subset of the FIA Database for Connecticut and then subset the database to only include observations necessary to compute estimates for the year 2018 (Figure).

Figure A.1: Example code to download and process data used in software validation.

```
## Load rFIA
library(rFIA)

## Download data
ct <- getFIA('CT')

## 2018 Subset
ct <- clipFIA(ct, mostRecent = FALSE, evalid = findEVALID(ct, year = 2018))
```

A.0.1 Live tree abundance (trees/acre)

EVALIDator

- Land Basis: Forestland
- Numerator: Tree Number
- Denominator: Area
- Estimate: Number of live trees (at least 1 inch d.b.h./d.r.c.), in trees, on forest land
- Evaluation: 092018N CONNECTICUT 2012;2013;2014;2015;2016;2017;2018
- Row Variable: EVALID

- Column Variable: EVALID

rFIA

Figure A.2: Example code to estimate live tree abundance

```
# Trees per acre
tpa_ct <- tpa(ct)
tpa_ct$TPA
```

A.0.2 Live tree basal area (sq.ft./acre)

EVALIDator

- Land Basis: Forestland

- Numerator: Tree basal area

- Denominator: Area

- Estimate: Basal area of live trees (at least 1 inch d.b.h./d.r.c.), in square feet, on forest land

- Evaluation: 092018N CONNECTICUT 2012;2013;2014;2015;2016;2017;2018

- Row Variable: EVALID

- Column Variable: EVALID

rFIA

Figure A.3: Example code to estimate live tree basal area

```
# Basal area per acre (BAA)
tpa_ct <- tpa(ct)
tpa_ct$BAA
```

A.0.3 Live tree merchantable volume (cu.ft./acre)

EVALIDator

- Land Basis: Forestland

- Numerator: Tree volume

- Denominator: Area

- Estimate: Net merchantable bole volume of live trees (at least 5 inch d.b.h./d.r.c.), in cubic feet, on forest land

- Evaluation: 092018N CONNECTICUT 2012;2013;2014;2015;2016;2017;2018

- Row Variable: EVALID

- Column Variable: EVALID

rFIA

Figure A.4: Example code to estimate live tree merchantable volume.

```
# Net volume per acre
bio_ct <- biomass(ct)
bio_ct$NETVOL_ACRE
```

A.0.4 Live tree sawlog volume (cu.ft./acre)

EVALIDator

- Land Basis: Forestland

- Numerator: Tree volume

- Denominator: Area

- Estimate: Net sawlog volume of live trees, in cubic feet, on forest land

- Evaluation: 092018N CONNECTICUT 2012;2013;2014;2015;2016;2017;2018

- Row Variable: EVALID

- Column Variable: EVALID

rFIA

Figure A.5: Example code to estimate live tree saw log volume.

```
# Sawlog volume per acre
bio_ct <- biomass(ct)
bio_ct$SAWVOL_ACRE
```

A.0.5 Live tree aboveground biomass (tons/acre)

EVALIDator

- Land Basis: Forestland

- Numerator: Tree dry weight

- Denominator: Area

- Estimate: Aboveground biomass of live trees (at least 1 inch d.b.h./d.r.c.), in short tons, on forest land

- Evaluation: 092018N CONNECTICUT 2012;2013;2014;2015;2016;2017;2018

- Row Variable: EVALID

- Column Variable: EVALID

rFIA

Figure A.6: Example code to estimate live tree aboveground biomass

```
# Sawlog volume per acre
bio_ct <- biomass(ct)
bio_ct$BIO_AG_ACRE
```

A.0.6 Live tree aboveground carbon (tons/acre)

EVALIDator

- Land Basis: Forestland

- Numerator: Tree carbon

- Denominator: Area

- Estimate: Aboveground carbon of live trees (at least 1 inch d.b.h./d.r.c.), in short tons, on forest land

- Evaluation: 092018N CONNECTICUT 2012;2013;2014;2015;2016;2017;2018

- Row Variable: EVALID

- Column Variable: EVALID

rFIA

Figure A.7: Example code to estimate live tree carbon

```
# Sawlog volume per acre
bio_ct <- biomass(ct)
bio_ct$CARB_AG_ACRE
```

A.0.7 Annual net biomass growth (tons/acre/year)

EVALIDator

- Land Basis: Forestland

- Numerator: Annual net growth dry weight

- Denominator: Area

- Estimate: Average annual net growth of aboveground biomass of trees (at least 5 inch d.b.h./d.r.c.), in short tons, on forest land

- Evaluation: 092018Y CONNECTICUT 2012;2013;2014;2015;2016;2017;2018

- Row Variable: EVALID

- Column Variable: EVALID

rFIA

Figure A.8: Example code to estimate live tree biomass growth.

```
# Annual biomass growth per acre
vr_ct <- vitalRates(ct)
vr_ct$BIO_GROW_AC
```

A.0.8 Annual mortality (trees/acre/year)

EVALIDator

- Land Basis: Forestland

- Numerator: Annual mortality number

- Denominator: Area

- Estimate: Average annual mortality of trees (at least 5 inch d.b.h./d.r.c.), in trees, on forest land

- Evaluation: 092018Y CONNECTICUT 2012;2013;2014;2015;2016;2017;2018

- Row Variable: EVALID

- Column Variable: EVALID

rFIA

Figure A.9: Example code to estimate tree mortality.

```
# Annual mortality TPA
gm_ct <- growMort(ct)
gm_ct$MORT_TPA
```

A.0.9 Annual removals (trees/acre/year)

EVALIDator

- Land Basis: Forestland

- Numerator: Annual removal number

- Denominator: Area

- Estimate: Average annual removals of trees (at least 5 inch d.b.h./d.r.c.), in trees, on forest land

- Evaluation: 092018Y CONNECTICUT 2012;2013;2014;2015;2016;2017;2018

- Row Variable: EVALID

- Column Variable: EVALID

rFIA

Figure A.10: Example code to estimate tree removals.

```
# Annual removals TPA
gm_ct <- growMort(ct)
gm_ct$REMV_TPA
```

A.0.10 Coarse woody debris volume (cu.ft./acre)

EVALIDator

- Land Basis: Forestland

- Numerator: Down woody material volume

- Denominator: Area

- Estimate: Total volume of CWD, in cubic feet, on forest land

- Evaluation: 092018N CONNECTICUT 2012;2013;2014;2015;2016;2017;2018

- Row Variable: EVALID

- Column Variable: EVALID

rFIA

A.0.11 Coarse woody debris biomass (tons/acre)

EVALIDator

Figure A.11: Example code to estimate coarse woody debris volume.

```
# CWD volume
dwm_ct <- dwm(ct)
dwm_ct$VOL_ACRE[dwm_ct$FUEL_TYPE == '1000HR']
```

- Land Basis: Forestland

- Numerator: Down woody material biomass

- Denominator: Area

- Estimate: Weight of CWD, in short tons, on forest land

- Evaluation: 092018N CONNECTICUT 2012;2013;2014;2015;2016;2017;2018

- Row Variable: EVALID

- Column Variable: EVALID

rFIA

Figure A.12: Example code to estimate coarse woody debris biomass.

```
# CWD biomass
dwm_ct <- dwm(ct)
dwm_ct$BIO_ACRE[dwm_ct$FUEL_TYPE == '1000HR']
```

A.0.12 Coarse woody debris carbon (tons/acre)

EVALIDator

- Land Basis: Forestland

- Numerator: Down woody material carbon

- Denominator: Area

- Estimate: Carbon of CWD, in short tons, on forest land

- Evaluation: 092018N CONNECTICUT 2012;2013;2014;2015;2016;2017;2018

- Row Variable: EVALID

- Column Variable: EVALID

rFIA

Figure A.13: Example code to estimate coarse woody debris carbon.

```
# CWD carbon
dwm_ct <- dwm(ct)
dwm_ct$CARB_ACRE[dwm_ct$FUEL_TYPE == '1000HR']
```

A.0.13 Total forest area ($acres\,x\,10^{-3}$)

EVALIDator

- Land Basis: Forestland

- Numerator: Area

- Denominator: None

- Estimate: Area in forestland, in acres

- Evaluation: 092018N CONNECTICUT 2012;2013;2014;2015;2016;2017;2018

- Row Variable: EVALID

- Column Variable: EVALID

rFIA

Figure A.14: Example code to estimate total forested area.

```
# Total Forest Area
fa_ct <- area(ct)
fa_ct$AREA_TOTAL
```

BIBLIOGRAPHY

BIBLIOGRAPHY

Henry D Adams and Thomas E Kolb. Drought responses of conifers in ecotone forests of northern arizona: tree ring growth and leaf δ 13 c. *Oecologia*, 140(2):217–225, 2004.

Henry D Adams and Thomas E Kolb. Tree growth response to drought and temperature in a mountain landscape in northern arizona, usa. *Journal of Biogeography*, 32(9):1629–1640, 2005.

Craig D Allen, Alison K Macalady, Haroun Chenchouni, Dominique Bachelet, Nate McDowell, Michel Vennetier, Thomas Kitzberger, Andreas Rigling, David D Breshears, EH Ted Hogg, et al. A global overview of drought and heat-induced tree mortality reveals emerging climate change risks for forests. *Forest ecology and management*, 259(4):660–684, 2010.

Michael B Ashcroft. Identifying refugia from climate change. *Journal of biogeography*, 37 (8):1407–1413, 2010.

Ernst Assmann. *The principles of forest yield study: studies in the organic production, structure, increment and yield of forest stands.* Elsevier, 2013.

Juliann E Aukema, Brian Leung, Kent Kovacs, Corey Chivers, Kerry O Britton, Jeffrey Englin, Susan J Frankel, Robert G Haight, Thomas P Holmes, Andrew M Liebhold, et al. Economic impacts of non-native forest insects in the continental united states. *PLoS one*, 6(9):e24587, 2011.

William A Bechtold, Paul L Patterson, et al. The enhanced forest inventory and analysis program-national sampling design and estimation procedures. *Gen. Tech. Rep. SRS-80. Asheville, NC: US Department of Agriculture, Forest Service, Southern Research Station. 85 p.*, 80, 2005. doi: 10.2737/SRS-GTR-80.

Santiago Beguería, Sergio M Vicente-Serrano, Fergus Reig, and Borja Latorre. Standardized precipitation evapotranspiration index (spei) revisited: parameter fitting, evapotranspiration models, tools, datasets and drought monitoring. *International Journal of Climatology*, 34(10):3001–3023, 2014.

Santiago Beguería and Sergio M. Vicente-Serrano. *SPEI: Calculation of the Standardised Precipitation-Evapotranspiration Index*, 2017. URL `https://CRAN.R-project.org/package=SPEI`. R package version 1.7.

David M Bell, John B Bradford, and William K Lauenroth. Early indicators of change: divergent climate envelopes between tree life stages imply range shifts in the western u nited s tates. *Global Ecology and Biogeography*, 23(2):168–180, 2014a.

David M Bell, John B Bradford, and William K Lauenroth. Mountain landscapes offer few opportunities for high-elevation tree species migration. *Global change biology*, 20(5): 1441–1451, 2014b.

Amy C Bennett, Nathan G McDowell, Craig D Allen, and Kristina J Anderson-Teixeira. Larger trees suffer most during drought in forests worldwide. *Nature Plants*, 1(10):15139, 2015.

Barbara J Bentz, Jacques Régnière, Christopher J Fettig, E Matthew Hansen, Jane L Hayes, Jeffrey A Hicke, Rick G Kelsey, Jose F Negrón, and Steven J Seybold. Climate change and bark beetles of the western united states and canada: direct and indirect effects. *BioScience*, 60(8):602–613, 2010.

Romain Bertrand, Jean-Claude Gégout, and Jean-Daniel Bontemps. Niches of temperate tree species converge towards nutrient-richer conditions over ontogeny. *Oikos*, 120(10): 1479–1488, 2011.

Christof Bigler, Daniel G Gavin, Charles Gunning, and Thomas T Veblen. Drought induces lagged tree mortality in a subalpine forest in the rocky mountains. *Oikos*, 116(12):1983–1994, 2007.

David D Breshears, Neil S Cobb, Paul M Rich, Kevin P Price, Craig D Allen, Randy G Balice, William H Romme, Jude H Kastens, M Lisa Floyd, Jayne Belnap, et al. Regional vegetation die-off in response to global-change-type drought. *Proceedings of the National Academy of Sciences*, 102(42):15144–15148, 2005.

Brian Buma, Carissa D Brown, Dan C Donato, Joseph B Fontaine, and Jill F Johnstone. The impacts of changing disturbance regimes on serotinous plant populations and communities. *BioScience*, 63(11):866–876, 2013.

Russell M Burns. *Silvics of North America: Conifers*. Number 654. US Department of Agriculture, Forest Service, 1990.

Elizabeth A Burrill, Andrea M Wilson, Jeffery A Turner, Scott A Pugh, James Menlove, Glenn Christiansen, Barbara L Conkling, and Winnie David. The forest inventory and analysis database: database description and user guide version 8.0 for phase 2. *Gen. Tech. Rep. RMRS-GTR-245. Fort Collins, CO: US Department of Agriculture, Forest Service, Rocky Mountain Research Station. 946 p.*, 245, 2018.

Michael J Case and David L Peterson. Fine-scale variability in growth climate relationships of douglas-fir, north cascade range, washington. *Canadian Journal of Forest Research*, 35 (11):2743–2755, 2005.

James S Clark, David M Bell, Matthew C Kwit, and Kai Zhu. Competition-interaction landscapes for the joint response of forests to climate change. *Global Change Biology*, 20 (6):1979–1991, 2014.

James S Clark, Louis Iverson, Christopher W Woodall, Craig D Allen, David M Bell, Don C Bragg, Anthony W D'Amato, Frank W Davis, Michelle H Hersh, Ines Ibanez, et al. The impacts of increasing drought on forest dynamics, structure, and biodiversity in the united states. *Global change biology*, 22(7):2329–2352, 2016.

Erin Conlisk, Cristina Castanha, Matthew J Germino, Thomas T Veblen, Jeremy M Smith, and Lara M Kueppers. Declines in low-elevation subalpine tree populations outpace growth in high-elevation populations with warming. *Journal of Ecology*, 105(5):1347–1357, 2017.

Joseph H Connell, JG Tracey, and Leonard J Webb. Compensatory recruitment, growth, and mortality as factors maintaining rain forest tree diversity. *Ecological monographs*, 54 (2):141–164, 1984.

Edward R Cook, Connie A Woodhouse, C Mark Eakin, David M Meko, and David W Stahle. Long-term aridity changes in the western united states. *Science*, 306(5698):1015–1018, 2004.

Kimberley T Davis, Solomon Z Dobrowski, Philip E Higuera, Zachary A Holden, Thomas T Veblen, Monica T Rother, Sean A Parks, Anna Sala, and Marco P Maneta. Wildfires and climate change push low-elevation forests across a critical climate threshold for tree regeneration. *Proceedings of the National Academy of Sciences*, 116(13):6193–6198, 2019.

Margaret B Davis and Ruth G Shaw. Range shifts and adaptive responses to quaternary climate change. *Science*, 292(5517):673–679, 2001.

R Justin DeRose and James N Long. Factors influencing the spatial and temporal dynamics of engelmann spruce mortality during a spruce beetle outbreak on the markagunt plateau, utah. *Forest Science*, 58(1):1–14, 2012.

Solomon Z Dobrowski, Alan K Swanson, John T Abatzoglou, Zachary A Holden, Hugh D Safford, Mike K Schwartz, and Daniel G Gavin. Forest structure and species traits mediate projected recruitment declines in western us tree species. *Global Ecology and Biogeography*, 24(8):917–927, 2015.

Christopher R Dolanc, James H Thorne, and Hugh D Safford. Widespread shifts in the demographic structure of subalpine forests in the sierra nevada, california, 1934 to 2007. *Global Ecology and Biogeography*, 22(3):264–276, 2013.

Francis H Eyre. Forest cover types. *Washington, DC: Society of American Foresters*, 1980.

Songlin Fei, Johanna M Desprez, Kevin M Potter, Insu Jo, Jonathan A Knott, and Christopher M Oswalt. Divergence of species responses to climate change. *Science Advances*, 3 (5):e1603055, 2017.

Jerry F Franklin, Thomas A Spies, Robert Van Pelt, Andrew B Carey, Dale A Thornburgh, Dean Rae Berg, David B Lindenmayer, Mark E Harmon, William S Keeton, David C Shaw, et al. Disturbances and structural development of natural forest ecosystems with silvicultural implications, using douglas-fir forests as an example. *Forest Ecology and Management*, 155(1-3):399–423, 2002.

Tracey S Frescino, Paul L Patterson, Gretchen G Moisen, and Elizabeth A Freeman. Fiesta—an r estimation tool for fia analysts, 2015. URL https://www.fs.usda.gov/treesearch/pubs/50184.

Alisa L Gallant, Andrew J Hansen, John S Councilman, Duane K Monte, and David W Betz. Vegetation dynamics under fire exclusion and logging in a rocky mountain watershed, 1856–1996. *Ecological Applications*, 13(2):385–403, 2003.

Andrew JR Gillespie. Rationale for a national annual forest inventory program. *Journal of Forestry*, 97(12):16–20, 1999. doi: 10.1093/jof/97.12.16.

Sara A Goeking. Disentangling forest change from forest inventory change: A case study from the us interior west. *Journal of Forestry*, 113(5):475–483, 2015.

Andrew N Gray, Thomas J Brandeis, John D Shaw, William H McWilliams, and Patrick Miles. Forest inventory and analysis database of the united states of america (fia). *In: Dengler, J.; Oldeland, J.; Jansen, F.; Chytry, M.; Ewald, J., Finckh, M.; Glockler, F.; Lopez-Gonzalez, G.; Peet, RK; Schaminee, J. HJ, eds. Vegetation databases for the 21st century. Biodiversity and Ecology. 4: 225-231.*, pages 225–231, 2012. doi: 10.7809/b-e. 00079.

Sarah Greenwood, Paloma Ruiz-Benito, Jordi Martínez-Vilalta, Francisco Lloret, Thomas Kitzberger, Craig D Allen, Rod Fensham, Daniel C Laughlin, Jens Kattge, Gerhard Bönisch, et al. Tree mortality across biomes is promoted by drought intensity, lower wood density and higher specific leaf area. *Ecology Letters*, 20(4):539–553, 2017.

Peter J Grubb. The maintenance of species-richness in plant communities: the importance of the regeneration niche. *Biological reviews*, 52(1):107–145, 1977.

Brian J Harvey, Daniel C Donato, and Monica G Turner. High and dry: Post-fire tree seedling establishment in subalpine forests decreases with post-fire drought and large stand-replacing burn patches. *Global Ecology and Biogeography*, 25(6):655–669, 2016.

Paul F Hessburg and James K Agee. An environmental narrative of inland northwest united states forests, 1800–2000. *Forest Ecology and Management*, 178(1-2):23–59, 2003.

Paul F Hessburg, James K Agee, and Jerry F Franklin. Dry forests and wildland fires of the inland northwest usa: contrasting the landscape ecology of the pre-settlement and modern eras. *Forest Ecology and Management*, 211(1-2):117–139, 2005.

Christ W. Hoffman, Robert L. Mathiasen, Richard W. Hofstetter, Mary Lou Fairweather, John D. Shaw, John W. Hanna, and Ned B. Klopfenstein. Survey for Armillaria by Plant Associations in Northern Arizona. *Journal of the Arizona-Nevada Academy of Science*, 45 (2):76 – 86, 2014. doi: 10.2181/036.045.0204.

Daniel G Horvitz and Donovan J Thompson. A generalization of sampling without replacement from a finite universe. *Journal of the American statistical Association*, 47(260): 663–685, 1952.

Kaicheng Huang, Chuixiang Yi, Donghai Wu, Tao Zhou, Xiang Zhao, William J Blanford, Suhua Wei, Hao Wu, Du Ling, and Zheng Li. Tipping point of a conifer forest ecosystem under severe drought. *Environmental Research Letters*, 10(2):024011, 2015.

Louis R Iverson, Anantha M Prasad, Stephen N Matthews, and Matthew Peters. Estimating potential habitat for 134 eastern us tree species under six climate scenarios. *Forest ecology and management*, 254(3):390–406, 2008.

Stephen T Jackson, Julio L Betancourt, Robert K Booth, and Stephen T Gray. Ecology and the ratchet of events: climate variability, niche dimensions, and species distributions. *Proceedings of the National Academy of Sciences*, 106(Supplement 2):19685–19692, 2009.

Peng Jiang, Hongyan Liu, Shilong Piao, Philippe Ciais, Xiuchen Wu, Yi Yin, and Hongya Wang. Enhanced growth after extreme wetness compensates for post-drought carbon loss in dry forests. *Nature communications*, 10(1):1–9, 2019.

Jill F Johnstone, Craig D Allen, Jerry F Franklin, Lee E Frelich, Brian J Harvey, Philip E Higuera, Michelle C Mack, Ross K Meentemeyer, Margaret R Metz, George LW Perry, et al. Changing disturbance regimes, ecological memory, and forest resilience. *Frontiers in Ecology and the Environment*, 14(7):369–378, 2016.

Paul A Klockow, Jason G Vogel, Christopher B Edgar, and Georgianne W Moore. Lagged mortality among tree species four years after an exceptional drought in east texas. *Ecosphere*, 9(10):e02455, 2018.

Kathryn W Kromroy, Jennifer Juzwik, Paul Castillo, and Mark H Hansen. Using forest service forest inventory and analysis data to estimate regional oak decline and oak mortality. *Northern journal of applied forestry*, 25(1):17–24, 2008.

Jonathan Lenoir, Jean-Claude Gégout, Jean-Claude Pierrat, Jean-Daniel Bontemps, and Jean-François Dhôte. Differences between tree species seedling and adult altitudinal distribution in mountain forests during the recent warm period (1986–2006). *Ecography*, 32 (5):765–777, 2009.

Heather E Lintz, Andrew N Gray, Andrew Yost, Richard Sniezko, Chris Woodall, Matt Reilly, Karen Hutten, and Mark Elliott. Quantifying density-independent mortality of temperate tree species. *Ecological indicators*, 66:1–9, 2016.

Yongqiang Liu, Scott L Goodrick, and John A Stanturf. Future us wildfire potential trends projected using a dynamically downscaled climate change scenario. *Forest Ecology and Management*, 294:120–135, 2013.

Zhihai Ma, Changhui Peng, Qiuan Zhu, Huai Chen, Guirui Yu, Weizhong Li, Xiaolu Zhou, Weifeng Wang, and Wenhua Zhang. Regional drought-induced reduction in the biomass carbon sink of canada's boreal forests. *Proceedings of the National Academy of Sciences*, 109(7):2423–2427, 2012.

František Máliš, Martin Kopeckỳ, Petr Petřík, Jozef Vladovič, Ján Merganič, and Tomáš Vida. Life stage, not climate change, explains observed tree range shifts. *Global change biology*, 22(5):1904–1914, 2016.

Sparkle L Malone, Anna W Schoettle, and Jonathan D Coop. The future of subalpine forests in the southern rocky mountains: Trajectories for pinus aristata genetic lineages. *PloS one*, 13(3), 2018.

Suzanne Bethers Marchetti, James J Worrall, and Thomas Eager. Secondary insects and diseases contribute to sudden aspen decline in southwestern colorado, usa. *Canadian Journal of Forest Research*, 41(12):2315–2325, 2011.

Ronald E. McRoberts and Patrick D. Miles. *United States of America*, pages 829–842. Springer International Publishing, Cham, 2016. ISBN 978-3-319-44015-6. doi: 10.1007/978-3-319-44015-6_45.

Ronald E McRoberts, William A Bechtold, Paul L Patterson, Charles T Scott, and Gregory A Reams. The enhanced forest inventory and analysis program of the usda forest service: Historical perspective and announcement of statistical documentation. *Journal of Forestry*, 103(6):304–308, 2005a.

Ronald E. McRoberts, Geoffrey R. Holden, Mark D. Nelson, Greg C. Liknes, Warren K. Moser, Andrew J. Lister, Susan L. King, Elizabeth B. LaPoint, John W. Coulston, W. Brad Smith, and Gregory A. Reams. Estimating and Circumventing the Effects of Perturbing and Swapping Inventory Plot Locations. *Journal of Forestry*, 103(6):275–279, 09 2005b. ISSN 0022-1201. doi: 10.1093/jof/103.6.275. URL https://doi.org/10.1093/jof/103.6.275.

Constance I Millar, David A Charlet, Robert D Westfall, John C King, Diane L Delany, Alan L Flint, and Lorraine E Flint. Do low-elevation ravines provide climate refugia for subalpine limber pine (pinus flexilis) in the great basin, usa? *Canadian Journal of Forest Research*, 48(6):663–671, 2018.

Maria N Miriti. Ontogenetic shift from facilitation to competition in a desert shrub. *Journal of Ecology*, 94(5):973–979, 2006.

Vicente J Monleon and Heather E Lintz. Evidence of tree species' range shifts in a complex landscape. *PLoS One*, 10(1), 2015.

Georgianne W Moore, Christopher B Edgar, Jason G Vogel, Robert A Washington-Allen, Rosaleen G March, and Rebekah Zehnder. Tree mortality from an exceptional drought spanning mesic to semiarid ecoregions. *Ecological Applications*, 26(2):602–611, 2016.

Cameron Naficy, Anna Sala, Eric G Keeling, Jon Graham, and Thomas H DeLuca. Interactive effects of historical logging and fire exclusion on ponderosa pine forest structure in the northern rockies. *Ecological Applications*, 20(7):1851–1864, 2010.

Stephen W Pacala, Charles D Canham, John Saponara, John A Silander Jr, Richard K Kobe, and Eric Ribbens. Forest models defined by field measurements: estimation, error analysis and dynamics. *Ecological monographs*, 66(1):1–43, 1996.

Wesley Green Page and Michael James Jenkins. Mountain pine beetle-induced changes to selected lodgepole pine fuel complexes within the intermountain region. *Forest Science*, 53(4):507–518, 2007.

Zuzana Parobeková, Ján Pittner, Stanislav Kucbel, Milan Saniga, Michal Filípek, Denisa Sedmáková, Jaroslav Vencurik, and Peter Jaloviar. Structural diversity in a mixed spruce-fir-beech old-growth forest remnant of the western carpathians. *Forests*, 9(7):379, 2018.

Richard G Pearson and Terence P Dawson. Predicting the impacts of climate change on the distribution of species: are bioclimate envelope models useful? *Global ecology and biogeography*, 12(5):361–371, 2003.

Edzer Pebesma. Simple Features for R: Standardized Support for Spatial Vector Data. *The R Journal*, 10(1):439–446, 2018. doi: 10.32614/RJ-2018-009. URL `https://doi.org/10.32614/RJ-2018-009`.

Robert K Peet. Forest vegetation of the colorado front range. *Vegetatio*, 45(1):3–75, 1981.

Therese M Poland and Deborah G McCullough. Emerald ash borer: invasion of the urban forest and the threat to north america's ash resource. *Journal of Forestry*, 104(3):118–124, 2006.

PRISM Climate Group. Prism climate group, 2010. URL `http://www.prism.oregonstate.edu/`.

Scott A. Pugh, Jeffery A. Turner, Elizabeth A. Burrill, and Winnie David. *The Forest Inventory and Analysis Database: Population Estimation User Guide*. USDA Forest Service, Washington DC, USA, 2018. URL `https://www.fia.fs.fed.us/library/database-documentation/current/ver80/FIADB`.

Camille Py, John Bauer, Peter J Weisberg, and Franco Biondi. Radial growth responses of singleleaf pinyon (pinus monophylla) to wildfire. *Dendrochronologia*, 24(1):39–46, 2006.

R Core Team. *R: A Language and Environment for Statistical Computing*. R Foundation for Statistical Computing, Vienna, Austria, 2018a. URL `https://www.R-project.org/`.

R Core Team. *R: A Language and Environment for Statistical Computing*. R Foundation for Statistical Computing, Vienna, Austria, 2018b. URL `https://www.R-project.org/`.

Gerald E Rehfeldt, Dennis E Ferguson, and Nicholas L Crookston. Aspen, climate, and sudden decline in western usa. *Forest Ecology and Management*, 258(11):2353–2364, 2009.

Robin M Reich, John E Lundquist, and Kristina Hughes. Host-environment mismatches associated with subalpine fir decline in colorado. *Journal of forestry research*, 27(5):1177–1189, 2016.

Alexia A. Sabor, Volker C. Radeloff, Ronald E. McRoberts, Murray Clayton, and Susan I. Stewart. Adding uncertainty to forest inventory plot locations: effects on analyses using geospatial data. *Canadian Journal of Forest Research*, 37(11):2313–2325, 2007. doi: 10.1139/X07-067. URL `https://doi.org/10.1139/X07-067`.

Josep M Serra-Diaz, Robert M Scheller, Alexandra D Syphard, and Janet Franklin. Disturbance and climate microrefugia mediate tree range shifts during climate change. *Landscape Ecology*, 30(6):1039–1053, 2015.

Josep M Serra-Diaz, Janet Franklin, Whalen W Dillon, Alexandra D Syphard, Frank W Davis, and Ross K Meentemeyer. California forests show early indications of both range shifts and local persistence under climate change. *Global Ecology and Biogeography*, 25(2): 164–175, 2016.

W Brad Smith. Forest inventory and analysis: a national inventory and monitoring program. *Environmental pollution*, 116:S233–S242, 2002.

Hunter Stanke, Andrew O Finley, Aaron S Weed, Brian F Walters, and Grant M Domke. rfia: An r package for estimation of forest attributes with the us forest inventory and analysis database. *Environmental Modelling & Software*, page 104664, 2020.

Camille S Stevens-Rumann, Kerry B Kemp, Philip E Higuera, Brian J Harvey, Monica T Rother, Daniel C Donato, Penelope Morgan, and Thomas T Veblen. Evidence for declining forest resilience to wildfires under climate change. *Ecology letters*, 21(2):243–252, 2018.

Atticus EL Stovall, Herman Shugart, and Xi Yang. Tree height explains mortality risk during an intense drought. *Nature communications*, 10(1):1–6, 2019.

Charles Warren Thornthwaite. An approach toward a rational classification of climate. *Geographical review*, 38(1):55–94, 1948.

Luke Tierney, A. J. Rossini, Na Li, and H. Sevcikova. *snow: Simple Network of Workstations*, 2018. URL `https://CRAN.R-project.org/package=snow`. R package version 0.4-3.

Wade T Tinkham, Patrick R Mahoney, Andrew T Hudak, Grant M Domke, Mike J Falkowski, Chris W Woodall, and Alistair MS Smith. Applications of the united states forest inventory and analysis dataset: a review and future directions. *Canadian Journal of Forest Research*, 48(11):1251–1268, 2018.

Erkki Tomppo, Thomas Gschwantner, Mark Lawrence, Ronald E McRoberts, K Gabler, K Schadauer, C Vidal, A Lanz, G Ståhl, and E Cienciala. National forest inventories. *Pathways for Common Reporting. European Science Foundation*, pages 541–553, 2010.

Leo Törnqvist, Pentti Vartia, and Yrjö O Vartia. How should relative changes be measured? *The American Statistician*, 39(1):43–46, 1985.

Monica G Turner, Kristin H Braziunas, Winslow D Hansen, and Brian J Harvey. Short-interval severe fire erodes the resilience of subalpine lodgepole pine forests. *Proceedings of the National Academy of Sciences*, 116(23):11319–11328, 2019.

USDA Forest Service. Forest inventory and analysis national program, 2019a. URL `https://www.fia.fs.fed.us/`.

USDA Forest Service. Fia tools and data, 2019b. URL `https://www.fia.fs.fed.us/tools-data/`.

Phillip J Van Mantgem, Nathan L Stephenson, John C Byrne, Lori D Daniels, Jerry F Franklin, Peter Z Fulé, Mark E Harmon, Andrew J Larson, Jeremy M Smith, Alan H Taylor, et al. Widespread increase of tree mortality rates in the western united states. *Science*, 323(5913):521–524, 2009.

Marco Vanoni, Harald Bugmann, Magdalena Nötzli, and Christof Bigler. Quantifying the effects of drought on abrupt growth decreases of major tree species in switzerland. *Ecology and evolution*, 6(11):3555–3570, 2016.

Sergio M Vicente-Serrano, Santiago Beguería, Juan I López-Moreno, M Angulo, and A El Kenawy. A new global 0.5 gridded dataset (1901–2006) of a multiscalar drought index: comparison with current drought index datasets based on the palmer drought severity index. *Journal of Hydrometeorology*, 11(4):1033–1043, 2010.

Sergio M Vicente-Serrano, Célia Gouveia, Jesús Julio Camarero, Santiago Beguería, Ricardo Trigo, Juan I López-Moreno, César Azorín-Molina, Edmond Pasho, Jorge Lorenzo-Lacruz, Jesús Revuelto, et al. Response of vegetation to drought time-scales across global land biomes. *Proceedings of the National Academy of Sciences*, 110(1):52–57, 2013.

Hadley Wickham, Romain Francois, Lionel Henry, Kirill Müller, et al. dplyr: A grammar of data manipulation. *R package version 0.4*, 3, 2015.

Hadley Wickham, Jim Hester, and Winston Chang. *devtools: Tools to Make Developing R Packages Easier*, 2019. URL `https://CRAN.R-project.org/package=devtools`. R package version 2.1.0.

A Park Williams, Craig D Allen, Alison K Macalady, Daniel Griffin, Connie A Woodhouse, David M Meko, Thomas W Swetnam, Sara A Rauscher, Richard Seager, Henri D Grissino-Mayer, et al. Temperature as a potent driver of regional forest drought stress and tree mortality. *Nature climate change*, 3(3):292–297, 2013.

Carmen M Wong and Lori D Daniels. Novel forest decline triggered by multiple interactions among climate, an introduced pathogen and bark beetles. *Global change biology*, 23(5):1926–1941, 2017.

CW Woodall, K Zhu, JA Westfall, CM Oswalt, AW D'amato, BF Walters, and HE Lintz. Assessing the stability of tree ranges and influence of disturbance in eastern us forests. *Forest Ecology and Management*, 291:172–180, 2013.

James J Worrall, Suzanne B Marchetti, Leanne Egeland, Roy A Mask, Thomas Eager, and Brian Howell. Effects and etiology of sudden aspen decline in southwestern colorado, usa. *Forest Ecology and Management*, 260(5):638–648, 2010.

Ian J Wright, Peter B Reich, Mark Westoby, David D Ackerly, Zdravko Baruch, Frans Bongers, Jeannine Cavender-Bares, Terry Chapin, Johannes HC Cornelissen, Matthias Diemer, et al. The worldwide leaf economics spectrum. *Nature*, 428(6985):821–827, 2004.

Xiuchen Wu, Hongyan Liu, Xiaoyan Li, Philippe Ciais, Flurin Babst, Weichao Guo, Cicheng Zhang, Vincenzo Magliulo, Marian Pavelka, Shaomin Liu, et al. Differentiating drought legacy effects on vegetation growth over the temperate northern hemisphere. *Global change biology*, 24(1):504–516, 2018.

Kai Zhu, Christopher W Woodall, and James S Clark. Failure to migrate: lack of tree range expansion in response to climate change. *Global Change Biology*, 18(3):1042–1052, 2012.

Kai Zhu, Christopher W Woodall, Souparno Ghosh, Alan E Gelfand, and James S Clark. Dual impacts of climate change: forest migration and turnover through life history. *Global change biology*, 20(1):251–264, 2014.